Modeling age-related ocular media changes using the Farnsworth Munsell (FM) 100-Hue Test

by

Victor Opoku-Yamoah

A thesis

presented to the University of Waterloo

in fulfillment of the

thesis requirement for the degree of

Master of Science

in

Vision Science

Waterloo, Ontario, Canada, 2021

Author's Declaration

I hereby declare that I am the author of this thesis and that this reflects the true account of the outcome of my investigation. This is a true copy of the thesis, including any required final revisions, as accepted by my examiners.

I understand that my thesis may be made electronically available to the public.

Abstract

Introduction: Evaluation of chromatic discrimination can help diagnose and monitor diseases and disorders of the visual system; however, normal age-related changes can make diagnosing colour discrimination losses challenging. This problem holds especially for the Farnsworth Munsell 100 Hue test (FM100 Hue). Identifying specific contributions of areas of the visual system that influence the FM100 Hue performance could aid in establishing standardized interpretation of test results and help understand the mechanisms contributing to the age-related changes.

Purpose: This study aimed to examine the theoretical changes in the FM100 Hue scores produced by age-related changes in the ocular media transmittances. These changes were examined with, and without, a von Kries type chromatic adaptation to determine the role of this adaptation process on age-related changes in hue discrimination.

Materials and methods: We calculated the CIECAM02 chromaticity coordinates of the FM100 Hue caps for 32-year-old and 74-year-old as ideal observers. These values were then used to predict the ordering of the FM100 Hue caps. The chromaticity coordinates were based on the spectral distribution of Illuminant D65, the spectral reflectances of the individual caps, and the CIE 1931 2^{o} standard observer colour matching functions.

In calculating the values of the old observers, we modified the spectral distributions of the D65 light sources using Pokorny et al.'s and van de Kraats and van Norren's model of media transmittance to account for the relative change in transmittance from a 32-year-old observer to a 74-year-old observer. We also accounted for the decrease in retinal illumination in the older observers due to pupil miosis and the decrease in ocular media luminous transmittance.

The order of the caps was based on the minimum colour differences (ΔE) between nearby caps. The mean and standard deviation of the colour differences for each tray was calculated. The mean colour difference was also determined for the caps in the blue-yellow (BY) and red-green (RG) quadrants.

Results: With complete and partial adaptation, the Total Error Score (TES) increased from 8 for the younger observer to12 for both older observer models of media transmittance. The ordering for the caps along the blue-yellow axis was unchanged from the younger observer. Without adaptation, the error score for the older observer model increased further. The increase was primarily for caps along the red-green axis for van de Kraats and van Norren's model, whereas the increase for Pokorny et al.'s model was along both the red-green and blue-yellow axis.

The mean colour differences across trays for the young observer model were marginally larger than the old observer models for complete and partial adaptation. When the caps were grouped in the RG and BY quadrants, the mean differences for the older observers were still lower than the young observer. Differences between the BY and RG error scores were also larger for the older observers. Without adaptation, the mean colour differences for the older observer models were uniformly lower than with complete or partial adaptation.

Conclusion: The predicted effect of age-related changes in media transmittances on the ordering of the FM100 Hue test showed an increase in the TES, as expected. The increase, however, was primarily due to an increase in the RG partial error score, which disagrees with the psychophysical data showing a larger increase in the BY error score. This discrepancy suggests that age-related neural changes are also occurring, which is consistent with conclusions from other psychophysical studies. The two different models for age-related media changes produced similar changes in the FM100 error scores. Chromatic adaptation may compensate for age-related media changes.

Acknowledgements

I want to express profound appreciation to my Supervisor, Dr. Jeffery K. Hovis, for his dedicated support, guidance, and assistance in this journey. Truly, I am most grateful for all the funding and other financial privileges rendered to my family and me. I feel highly honored and privileged to have been under your tutelage to explore such an interesting area as Colour Vision Science. I am also thankful for the support and direction of my committee members, Dr. Daphne McCulloch and Dr. Zay Khan. Your unwavering mentorship, contributions, and encouragement have been monumental in achieving this feat. I would like to thank the School of Optometry and Vision Science, University of Waterloo, for granting me a research space and a congenial study environment.

Special thanks to Dr. Stephen Dain for allowing us to use his data.

I would also like to thank my family for their advice and support 'through thick and thin'. I pray that the good Lord would attend to us at the point of our need. God bless you.

Dedication

I humbly dedicate this work to my wonderful life partner, Gifty, and our precious son, Michael.

Thank you for your love and for making my life more fulfilling.

Table of Contents

List of Figures

List of Tables

Chapter 1

Introduction

1.1 Introduction to the chapter

Changes in human chromatic sensitivity throughout life have been a continuing area of both basic and clinical research. The basic research has helped provide a better understanding of the development of chromatic sensitivity from infancy to adulthood and the age-related changes that occur as adults age (Knoblauch et al., 2001; Paramei and Oakley, 2014). The clinical research paralleled the basic research to develop age-appropriate tests for children and establish age-related norms for specific colour vision tests so that losses in chromatic discrimination resulting from disorders and diseases affecting the visual system could be detected and monitored (Verriest, 1963; Verriest et al., 1982; Kinnear and Sahraie, 2002). This chapter overviews a model of colour perception, perceptual attributes, types of colour vision deficiencies, the changes in chromatic discrimination throughout life, and the Farnsworth Munsell Hue test (FM100).

1.2 Colour vision processing

The current perceptual models of colour vision combine the trichromatic theory with colour opponent processes (Hurvich and Jameson, 1955; Jameson and Hurvich, 1955; Guth, 1991; Guth, 1992; De Valois and De Valois, 1993). The trichromatic theory applies to the photoreceptor level while the opponent processes operate at subsequent neural levels. These models are often labelled as zone opponent colour vision models.

1.2.1 *Zone Opponent Colour Model*

The first level (or zone) contains the 3 cone photoreceptors. These are the long wavelength sensitive cones (L-cones), medium wavelength sensitive cones (M-cones), and short wavelength sensitive cones (S-cones). They are responsible for converting optical radiant energy into neural impulses. This initial process begins with the absorption of photons by the photopigment located in the outer segment of each cone. The photopigment is an opsin protein, and each type of photopigment has a different amino acid sequence which determines its absorption spectrum. The L-cone and M-cone opsins have a similar amino acid sequence, and so their individual spectral absorption functions overlap considerably relative to the S-cone photopigment absorption spectrum (Neitz et al., 1995; Neitz and Neitz, 2011). The cone response is based on the principle of univariance. This principle states that once an individual photopigment molecule absorbs a photon, the response of the cone is independent of wavelength (Rushton, 1972). That is, the response of a cone only depends on the number of photons absorbed. It follows from this principle that cones do not code colour because the responses of a cone at different wavelengths can be equated by adjusting the

number of photons to compensate for the spectral absorption characteristics of the photopigment. The principle of univariance also underlies colour matching (Lennie et al., 1993). Lights composed of different wavelengths and energy will look identical if the photoreceptor responses to the lights are identical.

The fact that individual cones do not code colour means that there must be some other mechanism that compares the responses of the cones to different stimuli in order to perceive colours. In the zone opponent colour models, these mechanisms are post-receptor channels. There may be multiple zones of the post-receptor channels (Guth, 1991; Guth, 1992; De Valois and De Valois, 1993), but in this review, we will describe the simpler single post-receptor level model based on the work of Jameson and Hurvich (1955) because it provides a reasonable first-order explanation of colour perception. The 3 photoreceptors feed into a red-green (R-G), a blue-yellow (B-Y) channel, and an achromatic (A) channel. The signal from R-G channel is red or green, whereas the B-Y channel signals blue and yellow. The achromatic channel signals black or white. The output of R-G channel can be calculated by subtracting the M cone response from the sum of the L-cone and S-cone responses (Jameson and Hurvich, 1955; Hurvich and Jameson, 1955). A positive output signals red while the negative signals green. The output of the B-Y channel is calculated by subtracting the sum of the L and M-cone responses from the S-cone response. A positive output signals blue and a negative output signals yellow. Hue is coded by the sign of the outputs and ratio of the two chromatic channels' responses. Zero output from either the R-G or B-Y channel means no hue of the respective channels is expressed (Jameson and Hurvich, 1955; Hurvich and Jameson, 1955; Gaska et al., 2016). For example, if the B-Y channel response is zero at 500 nm, then the light appears neither blue nor yellow. However, the output of the R-G channel is negative at 500 nm, which is the signal for green, and so light appears to be only green. Similarly, if the response of the R-G is zero, the spectral light will appear only blue (~470 nm) in the short wavelength region or yellow (~575 nm) in the long wavelength region of the spectrum. If the output of both the B-Y and R-G channels is zero, then the stimulus will appear white, grey, or black.

1.3 Colour attributes

The human visible spectrum spans from 380 nm to 780 nm. The corresponding colours from short to long wavelengths are often described as violet, indigo, blue, green, yellow, orange, and red. The spectrum does not contain desaturated colours such as pink, magenta, or purple, which arise from mixtures of several wavelengths (Fairchild, 2013). Regardless of the colour vision model, the appearance of colours is described by the following attributes of hue, lightness or brightness, saturation or chroma, and colourfulness. These attributes will be defined in the following sections.

1.3.1 *Hue*

Hue is defined as the attribute of visual perception to which an object appears to be similar to, or different, from the colours described as red, yellow, green, and blue (Fairchild, 2013). A chromatic colour has a hue, whereas an achromatic colour is without any hue and appears as black, white, or grey. Within the zone opponent colour model, hue can be described from a combination of colours – red, green, blue, and yellow. These four hues are often referred to as the unique or psychological primaries. These hues possess the uniquely inherent organization of two opposing hue pairs, i.e., red-green and blue-yellow; hence they cannot co-occur. That is, there is no "reddish-green" or "yellowish-blue" (Jameson and Hurvich, 1955; Hurvich and Jameson, 1955; Pokorny et al., 1979).

1.3.2 *Lightness and brightness*

Lightness is expressed as the brightness of an object relative to the brightness of a similarly illuminated white reference (CIE, 2020a). Brightness, on the other hand, is the perceived intensity of emitted, transmitted, or reflected light. That is, brightness is the perception of absolute intensity, whereas lightness is the perception of the relative brightness of an object (Fairchild, 2013). Simplistically, brightness and lightness are modeled by the response of the achromatic channel, although the chromatic channels can also contribute to brightness (Guth et al., 1980; Burns et al., 1982).

1.3.3 *Saturation, colourfulness, and chroma*

These three terms describe the magnitude of the chromatic response relative to some reference, which is usually an achromatic colour. Colourfulness is a general term describing the degree of chromaticness, usually referenced to a grey (CIE, 2020a). For a fixed wavelength, colourfulness usually increases as the luminance of the stimulus is increased. Saturation is the perceptual attribute in which the colourfulness of a stimulus is compared to a white of the same brightness. Chroma is the colourfulness of a stimulus relative to a white reference under the same illuminant. Within the context of the zone opponent models, these attributes represent the ratio of the total chromatic response divided by the reference achromatic response. Traditionally, hue, chroma, and lightness are used to describe surface colours or the colours of objects that reflect light, and hue, saturation, and brightness are used to describe the colours of objects that emit light (Fairchild, 2013).

1.4 Classification of abnormal colour vision

Age-related changes in colour vision often resemble mild-to-moderate congenital colour vision deficiencies, particularly the tritan colour vision defect (Pokorny et al., 1979). For this reason, the characteristics of colour vision deficiencies will be described. A colour vision deficiency is defined as the difficulty in perceiving colour differences and/or having colour matches that fall beyond the normal limits

(Pokorny et al., 1979). Colour vision deficiencies may also be referred to as colour blindness by the general public, although complete colour blindness, referred to as achromatopsia, is found among very few people. Achromats perceive colours in shades of grey, i.e., black, or white.

A colour vision deficiency can occur with or without associated defects in visual function. In terms of origin, colour vision deficiencies associated with other impairments of visual function (e.g., visual acuity loss) are referred to as acquired colour vision deficiencies. Most of these deficiencies occur well after birth, although several of the "acquired" deficiencies are hereditary, and a few may be present at birth (Pokorny et al., 1979). The severity of acquired colour vision defects may vary between the eyes, regress, or progress along with the underlying condition, and errors in colour discrimination are not always predictable. In contrast, congenital colour vision defects are always hereditary, and the visual system is otherwise normal, or any other visual defects are not associated with the colour vision defect. Congenital defects are bilateral, affect both eyes equally and are stable with predictable errors in colour discrimination throughout life (Pokorny et al., 1979). Congenital red-green defects affect a greater proportion of males (4% – 12%) than females (0.2% to 0.4%) due to their X-linked recessive mode of inheritance (Birch, 2012; Tekavcic Pompe and Stirn Kranjc, 2012).

Colour vision deficiencies can be classified based on the mechanism responsible for the abnormal colour matches. These mechanisms are absorption, alteration, and reduction. Absorption refers to altered pre-receptor filters, such as the crystalline lens and macular pigment, causing variation in colour matches and spectral sensitivities. The neural components are all intact without any functional defect. Absorption systems can be created by simply introducing a coloured filter before the eyes or changing the illuminance source (Pokorny et al., 1979). Alteration is a difference in one or more photopigments compared to those of a normal trichromat. The altered photopigment has a different absorption spectrum from normal, resulting in different amounts of the primaries needed to make a colour match relative to colour-normals. Reduction is a reduction in the number of different types, not a loss in the absolute number of photoreceptors. This process results in a loss in colour discrimination without a loss in visual acuity or visual field loss.

1.4.1 *Congenital colour vision defects*

Congenital colour vision defects are classified as either dichromatic or anomalous trichromatic based on the number of primaries an observer requires to make a colour match (Pokorny et al., 1979). A dichromat requires 2 coloured primaries, while an anomalous trichromat requires three primaries to match a reference colour. The distinction between normal and anomalous trichromats is that the proportions of the primaries required to obtain a match for anomalous trichromats are outside the range of the proportions required by

normal trichromats. The colour discrimination of dichromats and most of the anomalous trichromats is also reduced.

The congenital red-green colour vision defect is an X-linked recessive defect that involves the loss of chromatic discrimination along the red-green axis. This type of defect is the most common colour vision defect (Pokorny et al., 1979). The red-green defects can be divided into two types of dichromatic defects and two types of anomalous trichromacy. Protanopia is missing the L-cone photopigment in the dichromatic (reduction) forms, whereas deuteranopia is missing the M-cone photopigment. In both cases, the missing cone photopigment has been replaced with the remaining longer wavelength absorbing photopigment. For the protanope, the L-cone photopigment is replaced by the M-cone photopigment, whereas the M-cone photopigment is replaced by the L-cone photopigment in the deuteranope. In anomalous red-green trichromacy (alteration form), one of the photopigments has also been replaced, but this time by a hybrid photopigment. In protanomaly, the L-cone photopigment is replaced by a hybrid photopigment with a spectral response whose peak sensitivity is shifted to a shorter wavelength relative to the L-cone of a normal trichromat but longer than normal M-cone photopigment. In deuteranomaly, the M-cone photopigment has been replaced by a hybrid photopigment that has a spectral response shifted to a longer wavelength relative to the M-cone of a normal trichromat but shorter than the normal L-cone photopigment (Neitz and Neitz, 2000). The severity of the anomalous trichromats can vary from very mild to severe based on their loss in colour discrimination. The discrimination loss is related to the difference between the peaks of the middle and longer wavelength sensitive photopigments (Shevell et al., 1998). With a better understanding of the genetics and expression of the photopigments, the reduction model represents the limiting case of the alteration mechanism for red-green congenital defects. When the difference between the peaks of the middle and long wavelength sensitive cones is zero, it becomes a reduction form of colour vision defect.

A congenital tritan defect has a discrimination loss along the blue-yellow chromatic axis. It is a rare autosomal dominant defect in which the S-cone is non-functional in the reduced dichromatic (tritanopia) case, or the S-cone has an impaired function in the tritanomalous case (Neitz and Neitz, 2000; Neitz and Neitz, 2010).

1.4.2 *Acquired colour vision defects*

Acquired colour vision defects often manifest as loss of blue-yellow discrimination (Pokorny et al., 1979). The severity of this defect may vary from mild to severe based on how the accompanying visual disorder progresses. This tritan-type defect is also seen with age and results in confusion of blues and blue-greens, yellow, grey, violet, and pinks with purple-pinks. The loss is due to cataract formation, pupillary miosis, and receptor and post receptor changes that occur with age (Schneck et al., 2014). Although the blue-yellow defects are the most common, acquired colour vision defects are often classified into three groups. These

are Type I acquired red-green, Type II red-green and Type III blue-yellow acquired colour vision defects. Type I acquired red-green colour vision defects are characterized by a progressive deterioration of colour discrimination along the red-green axis. The defect is similar to a protan defect with an altered spectral luminosity function in which the wavelength of maximum sensitivity is shifted towards shorter wavelengths and the Rayleigh match is shifted towards the red primary (Verriest, 1963). They occur predominantly in retinal diseases and/or photoreceptor disorders that usually become manifest before adulthood. The prognosis for maintaining normal visual acuity is usually poor.

Type II acquired red-green defects also lead to deterioration in chromatic discrimination along the red-green axis. In the early stages, the defect is characterized by reduced saturation of coloured stimuli, and this progresses to form a neutral zone (in which colours appear grey near 500 nm). The neutral zone widens as the condition progresses. The Rayleigh match is often displaced toward the green primary (Pokorny et al., 1979). The condition is often characterized by involvement of the optic nerve in conditions such as optic atrophies, optic neuritis, or tumours of the optic nerve/ chiasm. This defect varies from moderate to severe in terms of chromatic sensitivity loss. The chromatic discrimination and visual acuity often follow the progression or regression of the underlying condition.

Type III acquired blue-yellow defect is associated with mild to moderate loss of chromatic discrimination along the blue-yellow axis. This defect is characterized in the early stages by the confusion of 'blue and green' colours. These defects occur mainly in age-related conditions such as cataracts, glaucoma, vascular disorders and age-related macular degeneration (Verriest, 1963; Pokorny et al., 1979).

1.5 Development and maturation of colour discrimination

1.5.1 *Development of chromatic sensitivity from birth to adolescence*

Figure 1.1 summarizes major colour vision milestones that occur throughout life. The changes from birth to adolescence will not be discussed in detail in this thesis. Briefly, none of the neurosensory structures, including the cones, are adult-like at birth. Associated with the immature neural structures is poor chromatic and achromatic discrimination. There is a fairly rapid improvement in chromatic discrimination during the first 4 years of life, which corresponds to the maturity of the retinal structures and additional development of the post-retinal structures (Hendrickson and Yuodelis, 1984; Knoblauch et al., 2001; Hendrickson et al., 2012; Barbur and Rodriguez-Carmona, 2015). After the age of 4 years, there is a further improvement in chromatic discrimination at a slower rate until discrimination reaches an optimum value near the age of 20 years (Verriest et al., 1982; Knoblauch et al., 2001; Kinnear and Sahraie, 2002).

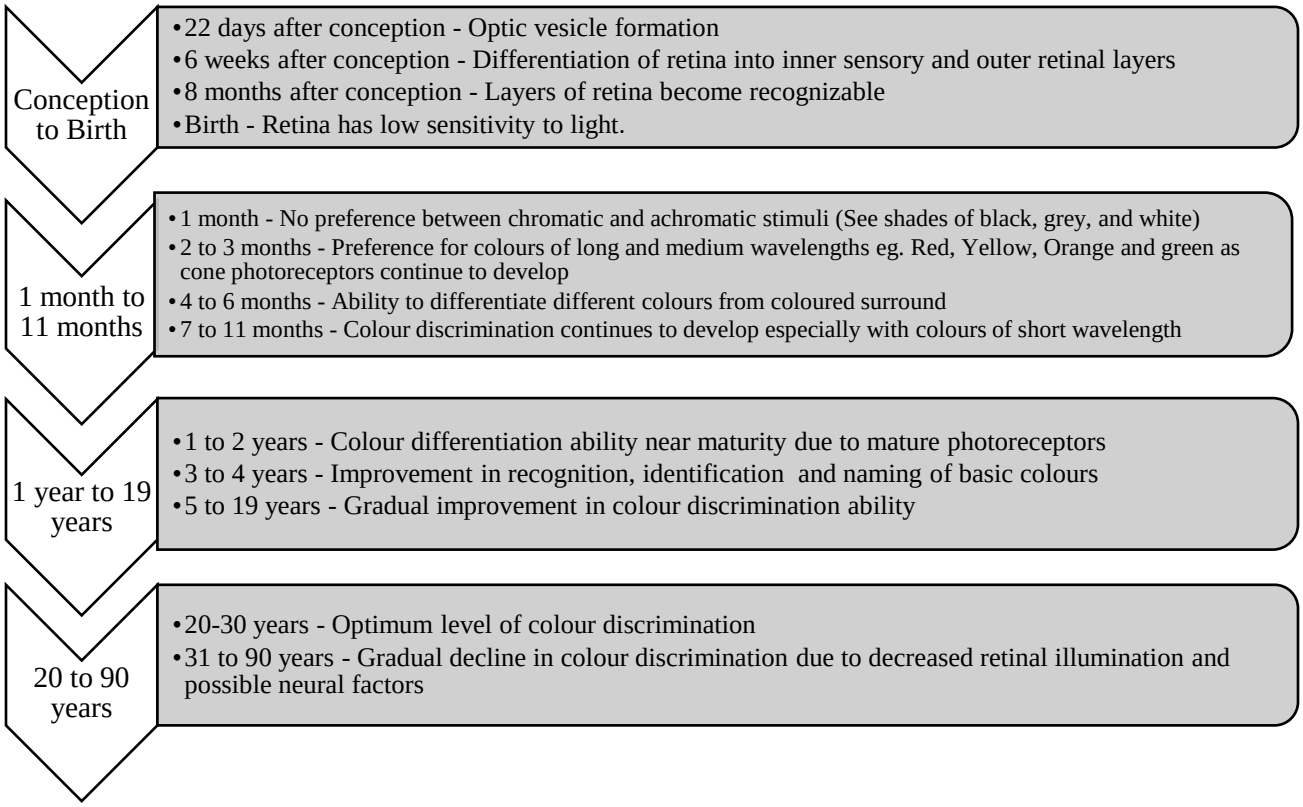

Figure 1.1: Timeline of the development of colour vision over the lifetime (Hendrickson and Yuodelis, 1984; Owsley, 2011; Hendrickson et al., 2012).

1.5.2 *Development of chromatic sensitivity - beyond adolescence*

Chromatic discrimination is optimum and remains relatively constant between 19 – 30 years (Verriest, 1963; Kinnear and Sahraie, 2002). Beyond the age of 30 years, there is a gradual decline in colour discrimination, especially along the blue-yellow axis (Verriest, 1963; Roy et al., 1991; Knoblauch et al., 2001; Schneck et al., 2014; Paramei and Oakley, 2014). The decline is associated with physiological changes in the ocular structures such as the pupil, cornea, crystalline lens, aqueous humour, vitreous humour, and retina. These changes and how they contribute to the reduction of chromatic discrimination are described in subsequent sections.

1.5.3 *Pupil size*

A major age-related change is a decrease in pupil size. This change is linear as a function of age, with a reduction rate ranging from 0.015mm to 0.043mm per year (Winn et al., 1994). The decrease in pupil diameter reduces the retinal illumination with age. Figure 1.2 shows the retinal illumination (i.e., E = L, Area of pupil) for a 32-year-old and 74-year-old observer for luminance levels ranging from 1 cd/m^2 to 1000 cd/m^2. The values were calculated from Watson and Yellot's equation for a 20-degree field of view and binocular viewing. There is a reduction of 0.69 in retinal illumination for the older eye at all photopic

light levels for this model. The reduction in retinal illumination could potentially decrease visual performance (Winn et al., 1994). Nevertheless, the reduction in pupil size with age improves depth of focus, minimizes lenticular light scatter, and reduces excessive retinal light exposure; thus, it could be beneficial for sharply focused retinal images among the aging population (Suryakumar and Allison, 2016). In terms of colour discrimination, a decrease in pupil size would reduce retinal illumination and increase TES on the FM100 Hue test (Dain et al., 1980; Knoblauch et al., 1987; Dain et al., 2004).

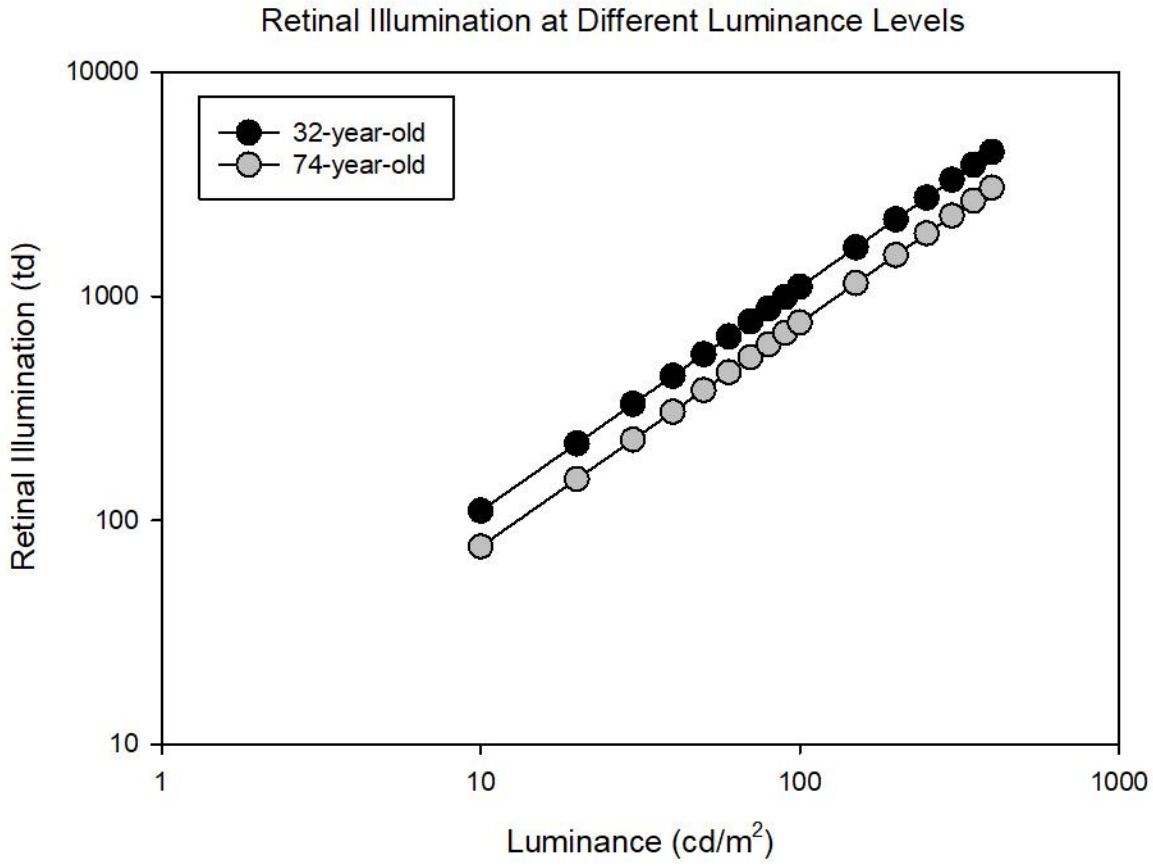

Figures 1.2: The plot represents the retinal illumination of a 32-year-old and 74-year-old at different light levels.

1.5.4 *Cornea*

The cornea is a prominent transparent media structure of the eye that transmits radiant energy in both the UV and the visible spectrum with a strong UV absorption below 310 nm (van de Kraats and van Norren, 2007). The total transmittance of the cornea does not change with age. The transparency of the cornea also remains intact unless scarring occurs at some point in time (van den Berg and Tan, 1994). Other changes in the cornea that could be influenced by aging, but do not directly affect colour discrimination include the

thickening of Descemet's membrane, changes in corneal astigmatism from 'with-the-rule' to 'against-the-rule', and corneal degenerations (Gipson, 2013).

1.5.5 *Aqueous and vitreous humour*

The aqueous is a transparent fluid containing proteins and other nutrients for the avascular cornea and lens. The aqueous has high transmittance in the visible region of the spectrum and this remains unaffected with aging (Boettner and Wolter, 1962). The high transmittance of the aqueous is attributed to the fact that it is composed mainly of water.

The vitreous humour is composed of a gel-like transparent fluid composed of predominantly water with collagen, proteins, and minerals as additional substances. It occupies the area behind the lens and in front of the retina and so it can affect the amount of light reaching the retina. The vitreous may occasionally experience liquefaction with advancing age, but this does not influence its transmittance unless the vitreous develops opacities such as floaters. Floaters usually produce localized shadows that vary with eye position and movement. Both the aqueous and vitreous humour have high, uniform transmittances (i.e., low optical densities) in the visible region of the spectrum (van de Kraats and van Norren, 2007).

1.5.6 *Crystalline lens*

Physiologically, the crystalline lens shows appreciable age-related changes in composition, form, and structure. There is a gradual age-related reduction in lens transmittance, with losses greater in the shorter wavelengths than the longer wavelengths (Pokorny et al., 1987; Weale, 1988; Beirne et al., 2008). The transmittance in the shorter wavelengths decreases by a factor of 0.48 – 0.54 between the ages of 32 years and 74 years, depending on the wavelength. The selective reduction in the spectral transmittance of the lens changes its appearance from being clear at birth to appearing yellow or brown in the seventh to eighth decades. This yellowing of the lens is often accompanied by cataracts that gradually develop with age. Cataracts could reduce image contrast due to light scattering and increased optical aberrations (Artal et al., 2003). Cataract formation also contributes to the reduction in retinal illumination (Owsley, 2011). Thus, the combination of the relative and absolute age-related changes in the lens results in decreased retinal illumination, especially at the shorter wavelengths. This leads to the decline in the S-cone pathway function, thereby producing a tritan-like colour vision loss with age (Werner, 2016).

1.5.7 *Retinal and neural changes*

The retina is the sensory layer in the back of the eyeball that receives light transmitted through the ocular media and begins neural processing as the information is transmitted back to the visual cortex. The cone photoreceptors, which are responsible for colour and fine resolution, are concentrated at the fovea. Beyond the central fovea, the retina is dominated by rod photoreceptors. In the anatomical macula (an area of about

6 mm or 20 degrees in diameter centred at fovea), the young adult rod to cone ratio is 9:1, whereas the ratio increases to 20:1 if the entire retina is considered. As we age, the number of rods decreases such that by the ninth decade, the number is reduced by 30% (Curcio et al., 1993). The loss is greatest within 3^{o} to 10^{o} of the fovea. Changes in rod photoreceptor density may contribute to decreased scotopic (rod-mediated) sensitivity among older adults (Curcio and Drucker, 1993; Owsley, 2011). This scotopic deficit is also associated with prolonged dark adaptation (Jackson et al., 2002). Further evidence suggests that the biochemical disruption in rhodopsin regeneration influences scotopic sensitivity loss with advancing age (Owsley, 2011).

In contrast, the number of cones remains relatively constant (Curcio et al., 1993). However, regional changes in the cone photopigments' optical densities occur and can affect the Rayleigh colour matches (Eisner et al., 1987; Swanson and Fish, 1996). There is a shift in the Rayleigh match towards the red primary as the field size is enlarged in young adults (Pokorny and Smith, 1976). The change in the match is attributed to a reduction in the optical density of the L and M cones due to the shorter outer segments outside of the fovea. The change occurs because the spectral absorption functions of the cones narrow so that the relative quanta absorption of the cones changes (Pokorny et al., 1979). This effect is diminished in older adults suggesting that the difference in outer segment length between the central and peripheral cones is less in older adults (Swanson and Fish, 1996). That is, the L- and M-cone outer segment lengths decrease with age, but not the peripheral cone outer segments. In eyes with Age-related Macular Degenerations (AMD), Elsner et al. (2002) found that the average L and M cone optical density was less among AMD patients than among age-matched normal subjects, but the decrease did not correlate with any change in visual acuity. Compared to the L- and M-cones, S-cones are non-random and irregular in distribution and are less dense in all locations of the retina, representing 0-15% of all cones at a given eccentricity (Ahnelt et al., 1987; Curcio et al., 1991; Volbrecht et al., 2000). Overall, the cone population is thought to be stable with aging (Gao and Hollyfield, 1992); however, S-cones appear to be more vulnerable to aging (Eisner et al., 1987; Haegerstrom-Portnoy, 1988; Curcio et al., 1991).

1.6 Farnsworth Munsell 100 Hue Test and Changes with Age

The Farnsworth Munsell 100 Hue test (FM100) is used to measure general hue discrimination in both clinical and research settings. The FM100 Hue test consists of 85 caps contained in four separate boxes (Figure 1.3). These caps differ by small increments in hue as they map out the complete hue circle. The caps are numbered in sequence according to hue. The loose caps are removed from the box, and the subject is asked to arrange the caps in a hue sequence to form a gradual increment in colour from one end (anchor)

of the box to the other. Alternative instructions are to place the loose cap in the box that is most similar in colour to the last one placed in the box. To determine the subjects colour discrimination quantitatively, the error score for each cap is calculated. The error score for a cap is calculated as the sum of the absolute difference between the number of a cap and the number of the two adjacent caps (on both sides). A value of 2 is subtracted so that a perfect arrangement would result in an error score of zero. These individual cap scores are summed to give the total error score (TES). The TES is a measure of hue discrimination of the subject (Farnsworth, 1949; Kinnear and Sahraie, 2002). Smith et al. (1985) recommend reporting the partial RG and BY error scores if additional information on hue discrimination along a particular axis is required (Smith et al., 1985). Such information is helpful in studying the effects of aging and other retinal diseases on chromatic discrimination (Kinnear and Sahraie, 2002; Beirne et al., 2008).

The cap error scores can be plotted on a polar plot. The radial (or angular) coordinates are the cap numbers, and the distance from the centre is the cap error score. These plots can reveal regions within the hue circle where discrimination is reduced. Individuals with congenital color vision deficiencies show characteristic patterns of error scores, which can help classify the type of defect (Kinnear, 1970).

The hue difference between adjacent caps is small, and so individuals with normal color vision often make errors. This property allows one to classify an individual's hue discrimination as high, average, or low based on age-related norms. This information can help evaluate candidates for quality control positions involving colour judgments, such as the paint and textile industries (Farnsworth, 1949).

The FM100 Hue test has also been a mainstay in assessing and evaluating acquired colour vision defects in the clinical setting due to its ability to measure fine hue discrimination for the entire hue circle (Pokorny et al., 1979). However, it is limited in its ability to differentiate mild cases of anomalous trichromacy from normal colour vision and distinguish between protan and deutan subjects (Dain, 2004).

1.6.1 *FM100 Hue Test and Age*

The performance of the FM100 Hue test is highly dependent on age (Verriest, 1963; Pinckers, 1980; Roy et al., 1991; Kinnear and Sahraie, 2002). The TES is high in children and decreases gradually to a minimum near 20 years and then increases steadily. The error pattern in young and older subjects usually mimics a tritan deficiency (Dain, 2004).

The higher error scores on the FM100 for children is often attributed to attentiveness, and/or poor comprehension on how to perform the test. However, these factors are likely superimposed on lower colour discrimination in children. Other studies which used objective or age-appropriate colour vision tests also reported lower colour discrimination in younger children, especially along the blue-yellow axis (Knoblauch et al., 2001; Barbur and Rodriguez-Carmona, 2015).

Figure 1.3: The Farnsworth Munsell 100 Hue test. From bottom to top, tray 1 is nominally red to red-orange, 2 is yellow to yellow-green, 3 is green to green-blue and 4 is indigo to indigo-magenta**.**

1.6 Study questions, aims and objectives

1.6.1 *Study questions*

Reduction in chromatic discrimination with age could be due to:

- Decreased transmittance of shorter wavelengths.
- Decreased retinal illumination.
- Neural changes.
- Any combination of the three.

This thesis will examine the theoretical effect of age-related changes in the ocular media transmittance for an ideal observer to determine the degree to which age-related changes in media transmittance influence hue discrimination. Because neural adaptation can counteract age-related ocular media changes (Ruddock, 1965), and adaptation itself could be affected by age, hue discrimination using the FM100 will be examined with, and without, adaptation.

1.6.2 *Study aims and objectives*

- To examine the theoretical changes in the FM100 Hue test scores produced by age-related changes in the ocular media transmittances for two different ideal observers. One observer is 32 years old, and the other is 74 years old.
- These changes will be examined with and without a von Kries type chromatic adaptation to determine the role that this adaptation process may have on age-related changes in hue discrimination (Fairchild, 2013).

Chapter 2

Media Transmittance Models

2.1 Introduction to the chapter

Changes in the crystalline lens transmittance with age is cited as the primary source of the age-related changes in the ocular media transmittance (Ruddock, 1965; Pokorny et al., 1987; Weale, 1988; van de Kraats and van Norren, 2007). Based on this hypothesis, Pokorny et al., reviewed the literature on lens transmittance and developed a model to account for the relative age-related changes in the lens transmittance. Twenty years later, van de Kraats and van Norren (2007) redid a literature review and developed a model for the age-related transmittance of the ocular media, excluding the macular pigmentation. In addition to including most of the ocular media, van de Kraats and van Norren expanded the wavelength range to include the UV region from 300 nm to 400 nm and the age range to less than 20 years. Both models of media transmittance will be used in this study to examine how age-related media changes affect the FM100 Hue test. This chapter will review the two models and discuss their differences. Because we will be using optical density, *D*, and transmittance, *t*, interchangeably, equation 2.1 shows the relationship between transmittance and optical density.

$$Density, D_\lambda = \log\left(\frac{1}{t_\lambda}\right) \qquad 2.1$$

2.2 Pokorny et al (1987) Lens Transmittance Model

Pokorny et al. (1987) suggested that two elements were affecting the lens transmittance. The first is a growth factor that is responsible for the increase in absorption of UV radiation with age. They hypothesized that this factor increases at a fast rate during the first two decades of life, but it is stable after 20 years. The second factor is an aging factor that is primarily responsible for the age-related increased absorption in the short-wavelength region of the visible spectrum. This factor represents the yellowing of the lens with age. Nevertheless, one equation incorporating these two factors was insufficient because of differences in the rate of change for subjects under 60 years and over 60 years. The data showed a 3-fold increase in the lens density changes at short wavelengths for subjects older than 60 years relative to the young adults.

Their equations for calculating the relative optical density (relative to 650 nm) at various wavelengths, D_λ are:

$$D_\lambda = D_{\lambda 1}[1 + 0.02(A - 32)] + D_{\lambda 2} \quad \text{for ages 20 – 60 years} \qquad 2.2$$

$$D_\lambda = D_{\lambda 1}[1.56 + 0.0667(A - 60)] + D_{\lambda 2} \quad \text{over the age of 60 years} \qquad 2.3$$

where A is age in years, $D_{\lambda 2}$ is the optical density at wavelength λ for the component that remains constant after the age of 20 years, and $D_{\lambda 1}$ is the optical density at wavelength λ for the component that changes with age. $D_{\lambda 1}$ and $D_{\lambda 2}$ are referenced to the lens density of a 32-year-old observer since that is the age referenced in Pokorny et al. This age is also near where the FM100 Hue scores are minimum (Verriest, 1963; Verriest et al., 1982; Kinnear and Sahraie, 2002). A 74-year-old observer was selected because that is the average age of cataract surgery in Canada (CSO, 2008). Figure 2.1 shows the relative optical density of the young adult and a 74-year-old observer. The range of wavelengths used in plotting the figures in this chapter was extended to 780 nanometers because the upper limit of wavelengths used to calculate the chromaticity coordinates of the caps and light sources was 780 nm.

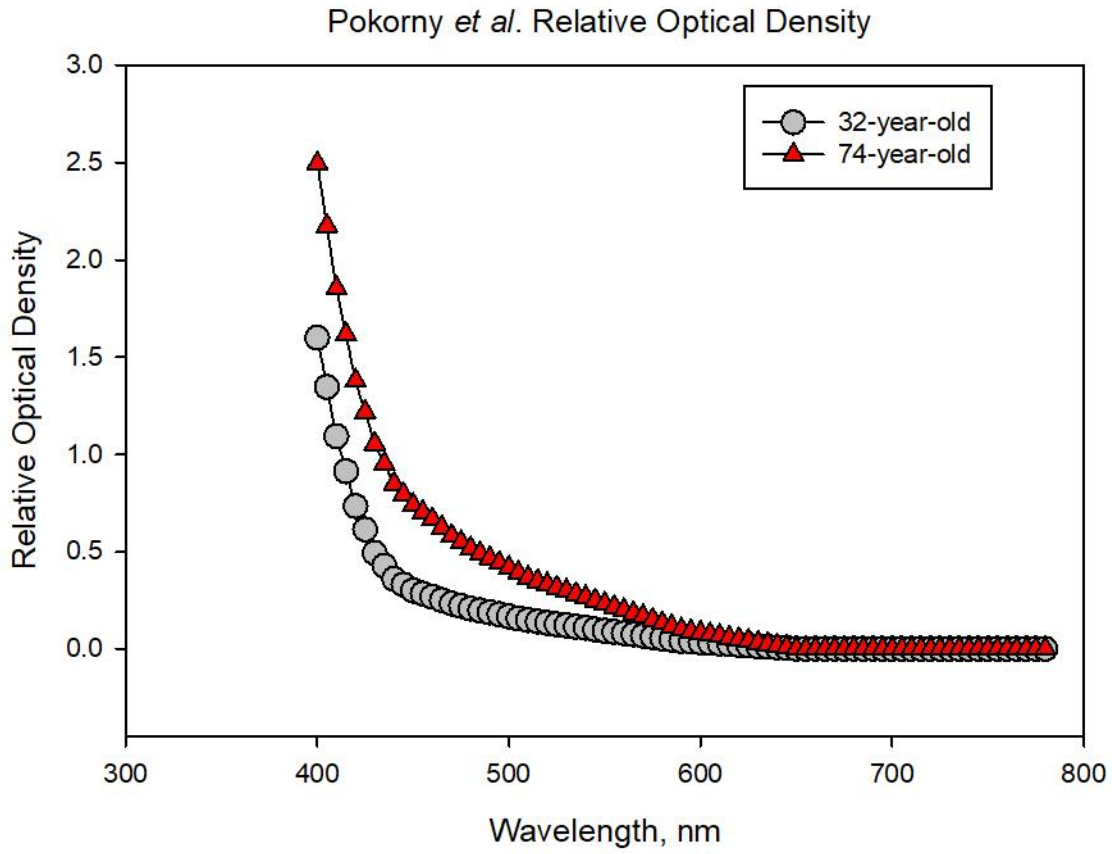

Figure 2.1: The relative optical density of the lenticular media using Pokorny et al (1987) lens transmittance equations. The filled circle and triangle symbols indicate the relative densities for young and old observers, respectively.

2.3 van de Kraats and van Norren (2007) Ocular Media Transmittance Model

The authors examined biological and psychophysical data in the literature to develop age-related functions that described the optical density of the human ocular media [$D_{media}(\lambda)$] from 300 nm to 700 nm, after

birth. Their equation is based on five components that are affected by age. The general form of the equation is:

$$D_{media}(\lambda) = \left[\sum_{i=1}^{5} d_i(age)\ x\ M_i(\lambda)\right] + d_{neutral} \qquad 2.4$$

where $D_{media}(\lambda)$ is the optical density of the ocular media at wavelength λ, M_i is a template of one of the media components, and d_i is an age-related scaling factor for M_i. The $d_{neutral}$ is a term to account for nonselective absorption by the media and light loss due to scattering by large molecules.

The age-related scaling factors have the general form of,

$$d_i = d_{i,0} + a_i \times age^2 \qquad 2.5$$

where $d_{i,0}$ is the density at age 0, a_i is the rate at which density changes with age in years^2, and *age* is the observer's age in years.

The components affecting media transmittance are Rayleigh scattering, tryptophan absorption, lens absorption of the young eye, lens absorption in the UV region of an older eye, and absorption of a lens of an older eye in the visible region. Except for the Rayleigh scatter template, the other templates are described by a Gaussian equation of the general form.

$$M_i(\lambda) = a \times exp(-[b \times (\lambda - \lambda_{max})]^2) \qquad 2.6$$

where $M_i(\lambda)$ is the density at wavelength λ, λ_{max}, is the wavelength of maximum density, b is the reciprocal of the function's width, and a is a scalar.

Rayleigh scatter is light loss due to scattering from small molecules that are present in all layers of the media. The equation for this template is,

$$M_{RL}(\lambda) = \left({}^{400}/_{\lambda}\right)^4 \qquad 2.7$$

Tryptophan is an essential amino acid found in most layers of the media (van de Kraats and van Norren, 2007). The molecule absorbs in the UV region (i.e., below 310 nm) and is included in the equation to account for age-related changes in UV absorption. The equation for the tryptophan absorption is,

$$M_{TP}(\lambda) = 10.68 \times exp\left(-([0.057 \times (\lambda - 273)]^2)\right) \qquad 2.8$$

where $M_{TP}(\lambda)$ is the density of the chromophore at wavelength λ.

The next three components model the age-related changes in the lens absorption. The three components are based on a different approach from the two components used by Pokorny et al. (1987). In the Pokorny et al. model, there was one base component and another to model age-related changes. In the van de Kraats and van Norren (2007) model, two components are related to the absorption of UV and short wavelength light, while the third component describes the absorption of the lens for medium-to-longer wavelengths of light.

The first lens component models absorption of the lens in the UVA and violet regions of the spectrum. The authors attribute this absorption to kynurenine derivatives present in the younger lens. Kynurenine is a yellowish coloured metabolite of tryptophan (van de Kraats and van Norren, 2007). The contribution of this component decreases with age because the amount of the kynurenine derivatives decreases with age (van de Kraats and van Norren, 2007). The equation for this template is,

$$M_{LY}(\lambda) = 2.13 \times exp\left(-([0.029 \times (\lambda - 370)]^2)\right) \qquad 2.9$$

where $M_{LY}(\lambda)$ is the density of the chromophores at wavelength λ.

According to van de Kraats and van Norren (2007), the decrease in the kynurenine derivatives with age is accompanied by an increase in an unspecified chromophore in the deeper layers of the old lens with major absorption in the UV. This chromophore absorbs radiation below 450 nm with a peak absorption in the 300 to 340 nm range. The equation for the template is,

$$M_{LOUV}(\lambda) = 11.95 \times exp\left(-([0.021 \times (\lambda - 325)]^2)\right) \qquad 2.10$$

where $M_{LOUV}(\lambda)$ is the density of the chromophores at wavelength λ.

The third lens component was required to model the lens transmittance properties in the visible region of the spectrum. This component was necessary because the other lens components and the Rayleigh scatter by the lens did not provide adequate fits to the data above 400 nm.

$$M_{LO}(\lambda) = 1.43 \times exp\left(-([0.008 \times (\lambda - 325)]^2)\right) \qquad 2.11$$

where $M_{LO}(\lambda)$ is density of the chromophores at wavelength λ.

The total density was then obtained by the sum of the respective functions of the media templates. For a 1-degree field, it was given as:

$$D_{media}(\lambda) = (0.446 + 0.000031 \times age^2) \times (400/\lambda)^4$$
$$+ 14.19 \times 10.68 \times exp\left(-([0.057 \times (\lambda - 273)]^2)\right)$$
$$+ (0.998 - 0.000063 \times age^2) \times 2.13 \times exp\left(-([0.029 \times (\lambda - 370)]^2)\right)$$
$$+ (0.059 + 0.000186 \times age^2) \times 11.95 \times exp\left(-([0.021 \times (\lambda - 325)]^2)\right)$$
$$+ (0.016 + 0.000132 \times age^2) \times 1.43 \times exp\left(-([0.008 \times (\lambda - 325)]^2)\right)$$
$$+ 0.111 \qquad 2.12$$

Figure 2.2 shows the optical density of a 32-year-old and 74-year-old observer.

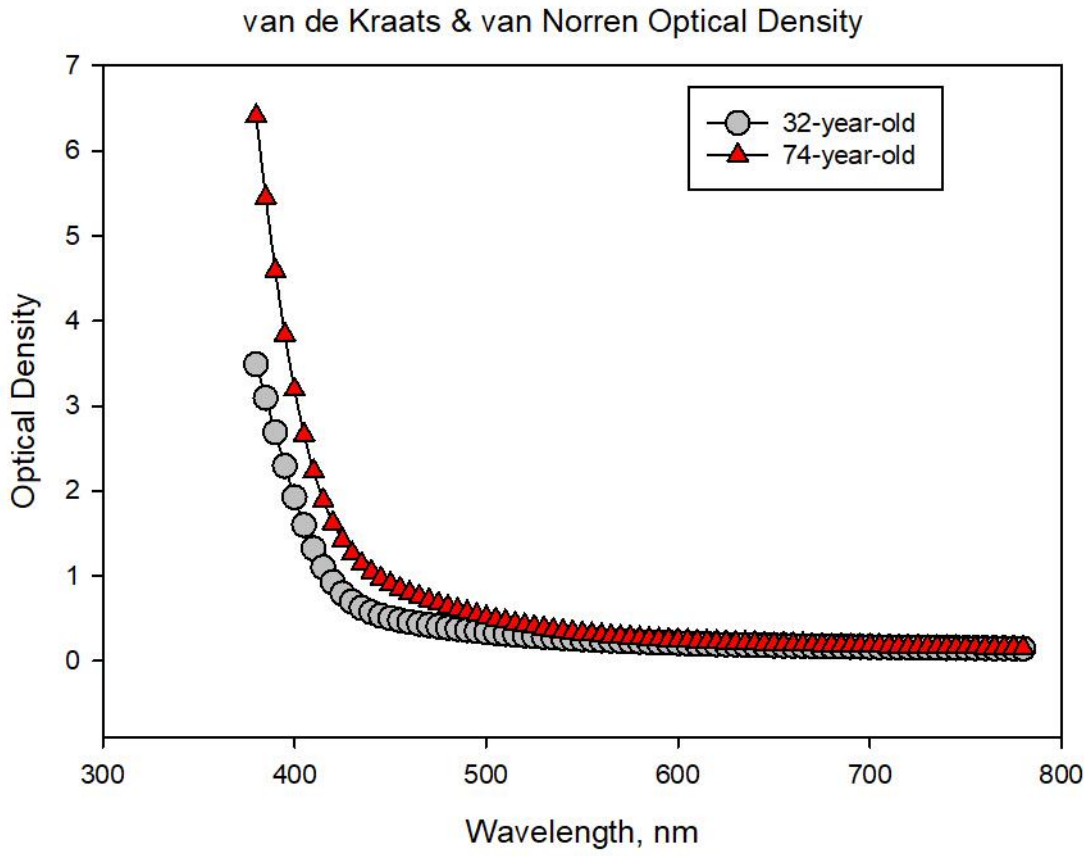

Figure 2.2: The optical density of the human ocular media using van de Kraats & van Norren (2007) ocular media transmittance model. The filled circle and triangle symbols indicate the optical densities for young and old observers of van de Kraats and van Norren, respectively.

2.4 Comparison of the two models

Figure 2.3 shows the relative optical density of the two models for the 32-year-old observer. Because the Pokorny et al. model is the density relative from 700 nm to zero, the van de Kraats and van Nooren values have also been normalized to 700 nm by subtracting 0.162. The relative optical densities of the young

observer for the two models are similar. The largest difference occurs between 400 nm and 500 nm, with the maximum difference of 0.16 density units at 400 nm. Figure 2.4 shows that the relative optical densities for van de Kraats and van Norren older observer were slightly greater than the optical density of Pokorny et al. observer, especially for wavelengths below 450 nm. The maximum difference at these shorter wavelengths was 0.536 at 400nm.

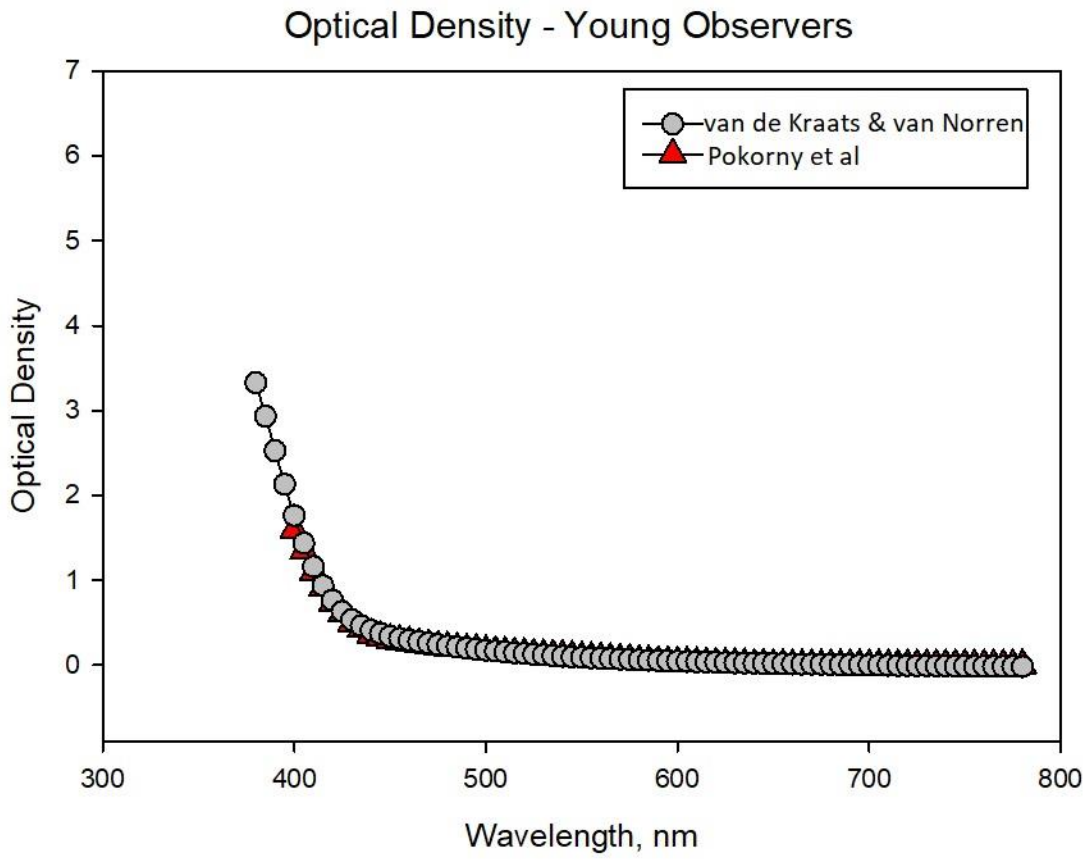

Figure 2.3: A plot of optical density against wavelength to compare the young observers of the van de Kraats and van Norren (2007) and Pokorny et al. (1987) models. The filled circles and triangles represent the optical densities of van de Kraats and van Norren (2007) and Pokorny et al. (1987), respectively. To equate the densities at the longer wavelengths, 0.16 was subtracted from the calculated densities for van de Kraats and van Norren's young observer.

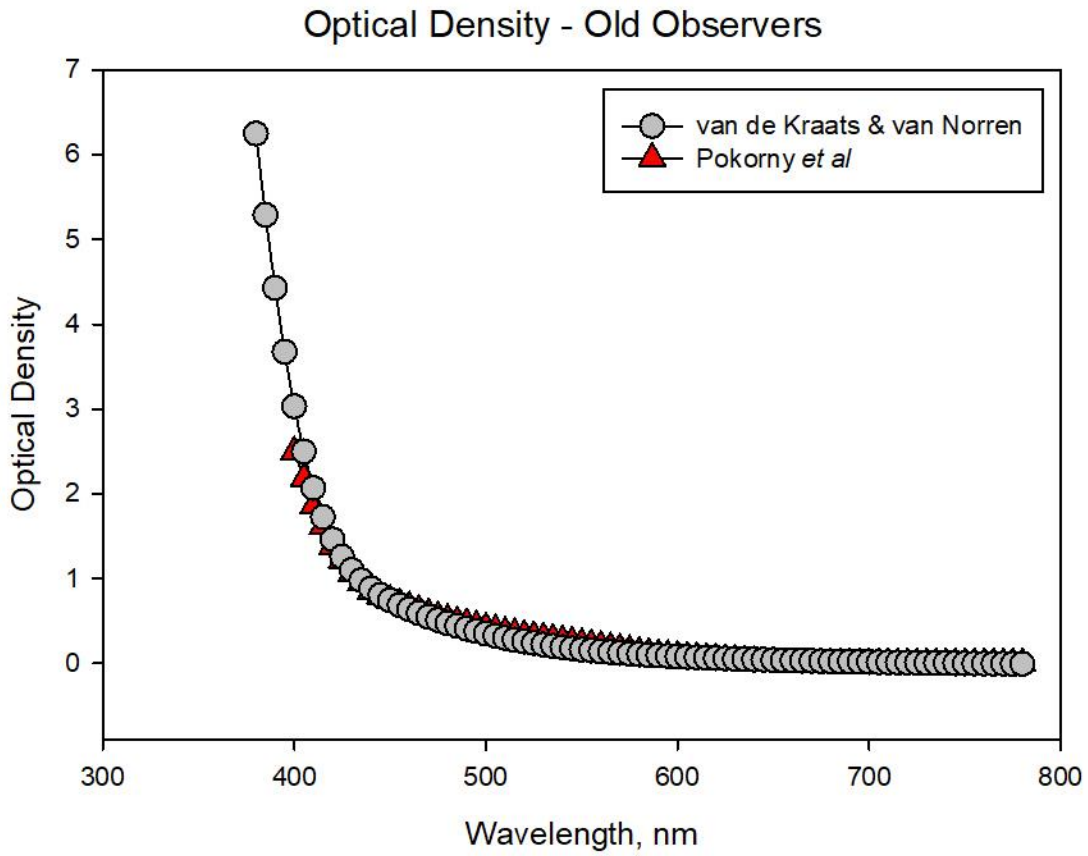

Figure 2.4: A plot of optical density against wavelength to compare the older observers of van de Kraats and van Norren (2007), and Pokorny et al. (1987). The filled circles and triangles represent the optical densities of van de Kraats and van Norren (2007) and Pokorny et al. (1987), respectively. To equate the densities at the longer wavelengths, 0.16 was subtracted from the calculated densities for van de Kraats and van Norren's old observer.

Comparison of the density plots for the two models showed that they were very similar to each other. This result was found by others in that their predicted results of age-related lens changes on colour vision were similar if either model was used (Shinomori et al., 2016). Nevertheless, because we are using the difference in optical density between the 32- and 74-year-old observers in our study, the differences between the ages for each model may be larger than the differences between models for a given age. Figure 2.5 shows the differences in optical density between 74 years and 32 years for the two models. Again, the difference values are similar. Nevertheless, the Pokorny et al. model has a larger difference between the two ages for wavelengths between 450 and 570 nm and a slightly smaller difference in the two ages near 400 nm.

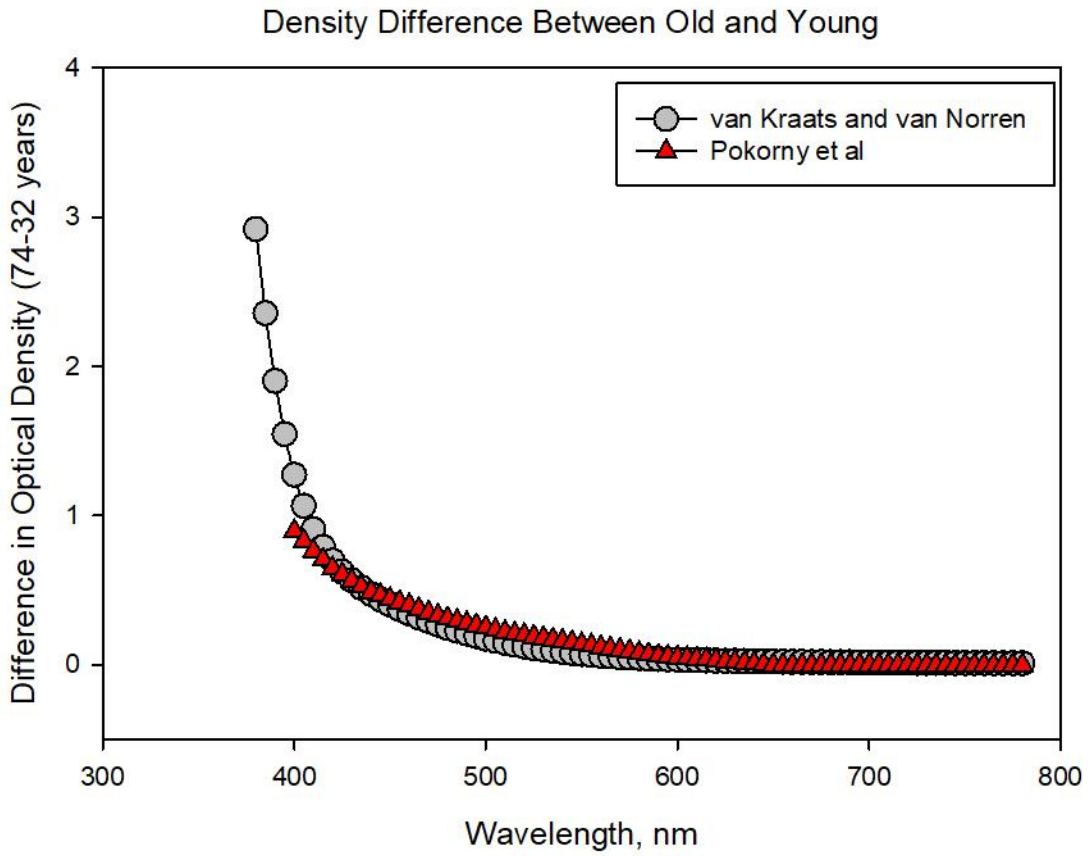

Figure 2.5: The difference in optical density between 74 and 32 years of age for Pokorny et al. (1987) lens transmittance model and van de Kraats and van Norren (2007) ocular media transmittance model.

Another way to look at the differences between the two models is to plot the chromaticity coordinates of the standard Illuminant D65 for the older observers in both models. The equations for calculating the chromaticity coordinates are given in Chapter 4. Briefly, the chromaticity coordinates of D65 for the older observers were calculated by multiplying the D65 spectral emittance by the change in the transmittance of the older observers relative to the young observer for each model. Figure 2.6 shows the results. The location of Illuminant A for a young observer is included for reference. Illuminant A is equivalent to a white incandescent source. As expected, the absorption of the short wavelength light in both models shifted D65 towards the yellow region of the CIE diagram. The degree of the shift is similar for both models, although the van de Kraats and van Norren's D65 for the older observer is shifted slightly to the green region of the diagram relative to the Pokorny et al. older observer. Figure 2.6 also shows a two-step MacAdam's ellipse for a nearby white (Wyszecki and Stiles, 1982). The area corresponds to 2 standard deviations of the colour matching data for the colour located at the center of the ellipse. If one colour was at the center of the ellipse and the other was at the edge, then the two colours would be noticeably different if they were displayed

adjacent to one another. Based on the size of the MacAdam's ellipse, the two D65 lights for the older observers would be noticeably different.

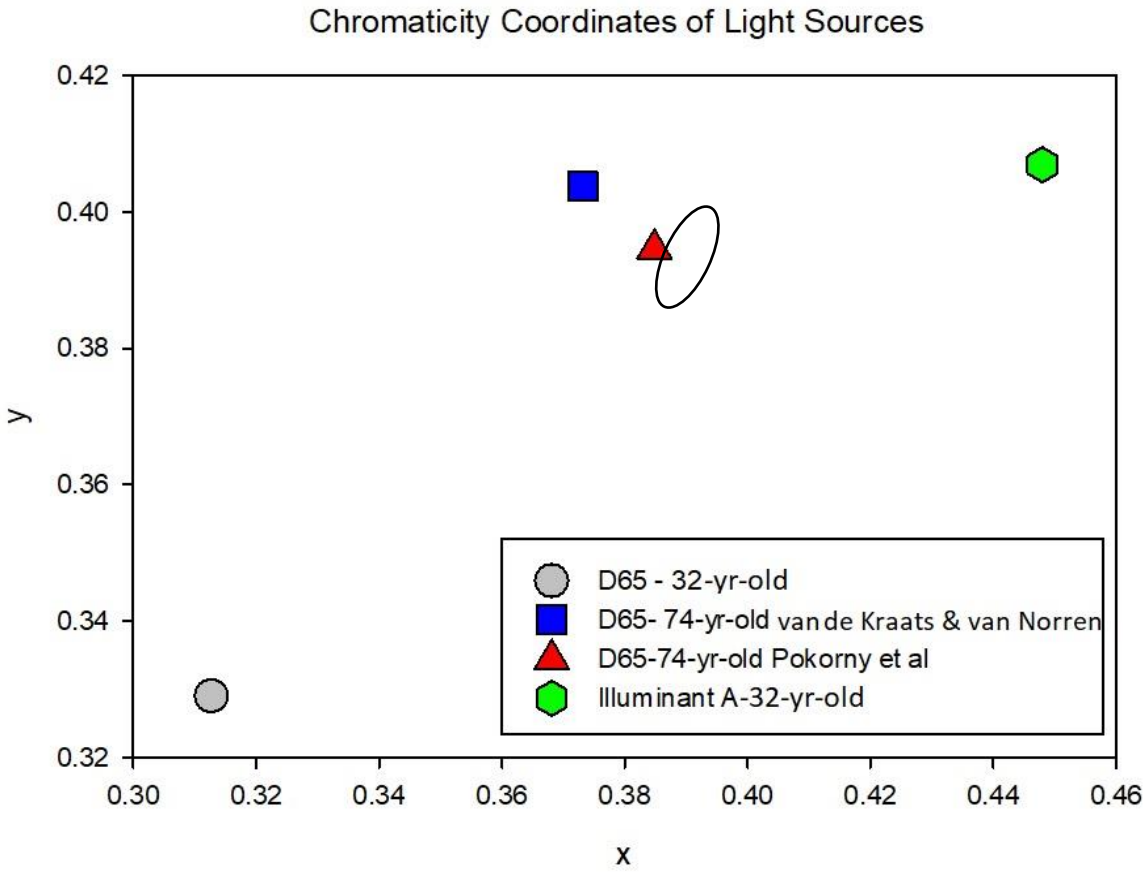

Figure 2.6: Plots of the chromaticity coordinates of the standard D65 light source for the young observer, the altered D65 light sources for the older observers, and Illuminant A for the young observer. The ellipse is a 2-step (i.e., 2 standard deviations) MacAdam's ellipse for a 2 degree field and dark surround for a young adult (Wyszecki and Stiles, 1982).

Chapter 3

Colour Appearance Model: CIECAM02

3.1 Introduction

The specification of colours has evolved over the last century from the 1931 x, y, z chromaticity system that specifies colours according to the relative amounts of the three primaries required to match the appearance of a colour, to more complex models that calculate the perceptual attributes of brightness, colourfulness, hue, lightness, chroma, and saturation. In evaluating the age-related media transmittance changes on the FM100, we wanted a model that included a factor to account for chromatic adaptation. As pointed out by Ruddock (1965), the changes in ocular media transmittance could be counteracted by chromatic adaptation. One such colour specification system is the CIECAM02. This model includes a chromatic adaptation process. It also allows us to examine how luminance can affect colour appearance. It has also been used to evaluate how different light sources affect the FM100 Hue ordering (Esposito, 2019). From a computation perspective, determining the effects of media transmittance on the FM100 Hue is equivalent to changing the light source.

3.2 CIECAM02

The CIECAM02 is a more recent version of a standardized colour appearance model. It is an improvement over the previous CIECAM97 with a linear chromatic adaptation transformation, improvements in accounting for the surround effects, improvements in the lightness parameter, and improvements in specifying saturation (CIE, 2004).

The first step in the CIECAM02 is the chromatic adaptation transform. Chromatic adaptation is described as the ability of the human visual system to adjust to widely varying colours of illumination in order to approximately preserve the appearance of object colours (Fairchild, 2013). This concept can be illustrated by considering a system that does not have the capacity for chromatic adaptation like photographic film optimized for daylight conditions. This film is designed for use in daylight exposures, but if one were to take photographs under incandescent illumination, the resulting pictures would have an unacceptable yellow-orange cast. This is due to the inability of the films to adjust the relative responsivities of its red, green and blue imaging layers in the way the human visual system adjusts the responsivities of its colour mechanisms (Fairchild, 2013). Humans perceive relatively little change in the colour of objects when the illumination is changed from natural daylight to incandescent lamps. The adaptation factor is applied at the cone level. Thus, it is necessary to first transform from CIE tristimulus values (XYZ) to cone responses.

In the CIECAM97's, this transformation was a more complex nonlinear process. The complexity made it more difficult to convert from CIECAM97 parameters back to the X, Y, Z tristimulus values. However,

additional research showed that using a simpler linear "cone space" with a von Kries chromatic adaptation transform would produce similar results (CIE, 2004). A 3x3 matrix, referred to as the CAT02 matrix (M_{CAT02}) was derived to convert the XYZ tristimulus values to a set of RGB tristimulus values for an equal energy balanced spectrum. These RGB functions are narrower compared with the corresponding L, M, and S cone spectral sensitivities. The matrix was derived to provide a linear space that provided a reasonable fit to the appearance of different data sets. The forward CAT02 matrix is shown in equation 3.1. The CIE 1931 standard 2° colorimetric observer was used to calculate tristimulus values of the stimulus and adapting stimulus.

$$\begin{bmatrix} R \\ G \\ B \end{bmatrix} = M_{CAT02} \begin{bmatrix} X \\ Y \\ Z \end{bmatrix} \qquad 3.1$$

where X, Y, Z are CIE tristimulus values and R, G, B, are tristimulus values for an equal energy Illuminant, where both R = G = B = 100 and X = Y = Z = 100.

$$M_{CAT02} = \begin{bmatrix} 0.7328 & 0.4296 & -0.1624 \\ -0.7036 & 1.6975 & 0.0061 \\ 0.0030 & 0.0136 & 0.9834 \end{bmatrix} \qquad 3.1a$$

The next stage is to apply the adaptation factor, *D,* which specifies the degree of adaptation for the white illuminant. It is computed as a function of the adapting luminance, L_A, and the surround's contribution to the degree of adaptation, *F* (Fairchild, 2013). The values for the surround parameters, including *F,* can be read from Table 1, which also specifies the values of the exponential nonlinearity, c, and the chromatic induction factor, N_c.

Table 1: Viewing condition parameters for different surrounds

Surround	**F**	**c**	**N_c**
Average	1.0	0.69	1.0
Dim	0.9	0.59	0.95
Dark	0.8	0.525	0.8

$$D = F\left[\left(\frac{1}{3.6}\right) e^{-(L_A + 42)/92}\right] \qquad 3.2$$

The *D* factor ranges from 1 signifying complete adaptation to 0 for no adaptation to the adapted white point. However, *D* rarely falls below 0.6 in practice for a dark surround and will exponentially converge to 1 for average surrounds with increasingly large values of L_A (Moroney et al., 2002a).

This adaptation transform is then applied to the individual tristimulus values to derive the adapted tristimulus responses, $R_c\, G_c\, B_c$.

$$Rc = \left[\left(Yw\ \frac{D}{Rw}\right) + (1 - D)\right] R \qquad 3.4$$

$$Gc = \left[\left(Yw\ \frac{D}{Gw}\right) + (1 - D)\right] G \qquad 3.5$$

$$Bc = \left[\left(Yw\ \frac{D}{Bw}\right) + (1 - D)\right] B \qquad 3.6$$

where the *w* subscript denotes the corresponding value for the adopted white light, and the *c* subscript denotes the stimuli values.

Viewing condition-dependent constants are then computed to obtain intermediate values necessary to proceed with CIECAM02 computations. The component F_L, the luminance-level adaptation factor, is calculated from equations 3.7 & 3.8. The factor *n* is the luminance factor of the background and ranges from 0 for a dark background and 1 for a background luminance equal to the adopted white point (Moroney et al., 2002a). It is then used to compute N_{bb} and $N_{cb,}$ which are background brightness induction factors, and *z*, a base exponent. The values of F_L and the constant, *k* are dependent on L_A, the luminance of adapting field, whereas the remaining variables are dependent on the background's relative luminance, Y_b.

$$k = \frac{1}{5L_A+1} \qquad 3.7$$

$$F_L = 0.2\, k^4(5L_A) + 0.1\,(1 - k^4)^2(5L_A)^{1/2} \qquad 3.8$$

$$n = \frac{Y_b}{Y_w} \qquad 3.9$$

$$N_{bb} = N_{cb} = 0.725\left(\frac{1}{n}\right)^{0.2} \qquad 3.10$$

$$z = 1.48 + \sqrt{n} \qquad 3.11$$

The adapted RGB tristimulus responses are converted to Hunt-Pointer Estevez (HPE) cone fundamentals. This is necessary to apply the post-adaptation non-linear compression because the HPE fundamentals more closely align with cone responsivities (Fairchild, 2013).

$$\begin{bmatrix} R' \\ G' \\ B' \end{bmatrix} = M_{HPE}\, M_{CAT02}^{-1} \begin{bmatrix} R_C \\ G_C \\ B_C \end{bmatrix} \quad 3.12$$

$$M_{HPE} = \begin{bmatrix} 0.38971 & 0.68898 & -0.07868 \\ -0.22981 & 1.18340 & 0.04641 \\ 0.00000 & 0.00000 & 1.00000 \end{bmatrix} \quad 3.12a$$

$$M_{CAT02}^{-1} = \begin{bmatrix} 1.096124 & -0.278869 & 0.182745 \\ 0.454369 & 0.473533 & 0.072098 \\ -0.009628 & -0.005698 & 1.015326 \end{bmatrix} \quad 3.12b$$

The post-adaptation non-linear compression is then applied to the output of equation 3.13 and given as,

$$R'_a = \frac{400(F_L R'/100)^{0.42}}{27.13+400(F_L R'/100)^{0.42}} + 0.1 \quad 3.13a$$

$$G'_a = \frac{400(F_L G'/100)^{0.42}}{27.13+400(F_L\, G'/100)^{0.42}} + 0.1 \quad 3.13b$$

$$B'_a = \frac{400(F_L B'/100)^{0.42}}{27.13+400(F_L B'/100)^{0.42}} + 0.1 \quad 3.13c$$

3.3 Opponent-colour dimensions

The output from equations 3.13 are used to generate preliminary Cartesian coordinates, a and b, which are used to compute a preliminary magnitude, t, (Moroney et al., 2002b). These are then used to work out colour appearance correlates or perceptual attributes.

$$a = R'_a - 12G'_a/11 + B'_a/11 \quad 3.16$$

$$b = \frac{1}{9}(R'_a + G'_a - 2B'_a) \quad 3.17$$

$$t = \frac{(50000/13)N_c N_{cb} e_t \sqrt{a^2+b^2}}{R'_a+G'_a+(21/20)B'_a} \quad 3.18$$

3.4 Hue

The hue angle, *h*, must be calculated in degrees, ranging from 0 to 360 degrees.

$$h = tan^{-1}(b/a) \quad 3.19$$

Next, *h* is used to compute the eccentricity factor, e_t. The eccentricity factor would be used as adjustment later in computing for chroma, *C*, together with some other factors. This eccentricity factor is required to improve the uniformity of the colour space.

$$e_t = \frac{1}{4}\left[cos\left(h\frac{\pi}{180} + 2\right) + 3.8\right] \quad 3.20$$

Hue quadrature or composition, *H*, specifies the stimulus using the four fundamental hues (red, green, yellow, and blue). For example, a colour with an *H* value of 50 will appear 50% red and 50% yellow. The value is determined by linear interpolation using the values in Table 2 below.

$$H = H_i + \frac{100(h - h_i)/e_i}{(h - h_i)/e_i + (h_{i+1} - h)/e_{i+1}} \quad 3.21$$

Table 2. Data for calculating hue quadrature from hue angle.

	Red	Yellow	Green	Blue	Red
i	1	2	3	4	5
h_i	20.14	90.00	164.25	237.53	380.14
e_i	0.8	0.7	1.0	1.2	0.8
H_i	0	100	200	300	400

3.5 Lightness

An initial achromatic response, *A* and lightness, *J*, are then computed. The achromatic response is computed using the weighted summation of nonlinear adapted cone responses altered with the brightness induction factor. The achromatic response for the white point, A_w, is computed in a similar manner (Fairchild, 2013).

$$A = \left[2R'_a + G'_a + \left(\frac{1}{20}\right)B'_a - 0.305\right]N_{bb} \quad 3.22$$

Lightness, *J*, specifies the achromatic response of the stimulus relative to the adopted white. It is calculated from the achromatic responses, *A*, the achromatic response for white, A_w, the surround factor, *c*, and the base exponent, *z*.

$$J = 100\left(\frac{A}{A_w}\right)^{cz} \quad 3.23$$

3.6 Brightness

Brightness, *Q*, is computed from lightness, *J*, the achromatic response for the white, A_w, the surround factor, *c*, and the luminance-level adaptation factor, F_L. It refers to the perceived luminance of emitted or reflected light.

$$Q = \left(\frac{4}{c}\right)\sqrt{J/100}(A_w + 4)F_L^{0.25} \quad 3.24$$

3.7 Chroma

The temporary magnitude quantity, *t* is used to compute for chroma, *C*, and colourfulness, *M*. Chroma is the colourfulness of a stimulus relative to a white reference under the same illumination.

$$C = t^{0.9}\sqrt{J/100}(1.64 - 0.29^{n})^{0.73} \quad 3.25$$

3.8 Colourfulness

Colourfulness, *M*, is computed by the mathematical combination of chroma, *C* and the fourth root of the luminance-level adaptation factor, F_L. It is the amount of chromaticness and increases with luminance up to extremely bright levels.

$$M = CF_L^{0.25} \quad 3.26$$

3.9 Saturation

Saturation, *S*, is the colourfulness of a stimulus relative to its brightness and is approximately constant at all luminance levels, except at very high levels. It is computed from colourfulness and brightness correlates as,

$$S = 100\sqrt{\frac{M}{Q}} \quad 3.27$$

Corresponding Cartesian coordinates a_i and b_i, are computed through simple coordinate transformation of chroma, *C*, colourfulness, *M*, or saturation, s, and hue, *h*. The subscript *C, M, and S* denote the specific correlates used to calculate the chromaticity coordinates. The subscripts' use helps avoid confusing these coordinates with the preliminary Cartesian coordinates shown in equations 3.16 & 3.17. We used the coordinates a_M, b_M because the small colour differences formula was based on them. However, the equivalent coordinates could be useful depending on the application being used.

$$a_C = C\ cos(h) \quad 3.28$$

$$b_C = C\ cos(h) \quad 3.29$$

$$a_M = M\ cos(h) \quad 3.30$$

$$b_M = M\ sin(h) \quad 3.31$$

$$a_S = S\ cos(h) \quad 3.32$$

$$b_S = S\ cos(h) \quad 3.33$$

Chapter 4

Materials and methods

4.1 Calculation of tristimulus values of FM100 Hue caps – Young observer

The first step in calculating the chromaticity coordinates of the FM100 caps in the CIECAM02 space is to calculate each cap's XYZ tristimulus values. These values are based on the spectral distribution of light source, the individual caps' spectral reflectances, and the CIE 1931 2° standard observer colour matching functions. The light source used for the young observer was Illuminant D65 (CIE, 2020b). The spectral reflectances of the FM100 caps in 5 nm intervals were graciously supplied by Dr. Stephen Dain. The procedure for measuring the reflectances is described in Dain et al., (2020).

The equations for calculating the tristimulus values for an individual cap are,

$$X_i = \sum_{\lambda=380}^{780} S_{e\lambda}\, r_{i,\lambda} x'_\lambda \Delta\lambda, \qquad 4.1$$

$$Y_i = \sum_{\lambda=380}^{780} S_{e\lambda}\, r_{i,\lambda} y'_\lambda \Delta\lambda, \qquad 4.2$$

$$Z_i = \sum_{\lambda=380}^{780} S_{e\lambda}\, r_{i,\lambda} z'_\lambda \Delta\lambda, \qquad 4.3$$

where $S_{e\lambda}$ is the relative spectral emittance of D65, $r_{i\lambda}$ is the spectral reflectance of cap i and x'_λ, y'_λ, z'_λ are the 1931 x' y' z' colour matching functions at wavelength λ. The Δλ is 5 nm. The relative spectral output of D65 was normalized so that the Y tristimulus value of D65 was 100. With this normalization, the Y_i represents the percent luminous reflectance of the cap.

4.2 Calculation of tristimulus values of FM100 Hue caps – Old observers

i. For the older observer, the spectral power distributions of the D65 light source were modified for the van de Kraats & van Norren and Pokorny's models to account for the relative change in spectral transmittance from 32-year-old to a 74-year-old. The media models are described in detail in Chapter 2. Briefly, Pokorny et al.'s equations for calculating the relative optical density at various wavelengths, D_λ are:

$$D_\lambda = D_{\lambda 1}[1 + 0.02(A - 32)] + D_{\lambda 2} \quad \text{for the 32-year-old} \qquad 4.5$$

$$D_\lambda = D_{\lambda 1}[1.56 + 0.0667(A - 60)] + D_{\lambda 2} \quad \text{for the 74-year-old} \qquad 4.6$$

where A is age in years, $D_{\lambda 2}$ is the optical density at wavelength λ for the component that remains constant after the age of 20 years, and $D_{\lambda 1}$ is the optical density at wavelength λ for the component that changes with age. The range of wavelength used for this model was 400 – 780 nm.

ii. van de Kraats and van Norren's equation for calculating the optical density has the general form of:

$$D_{media}(\lambda) = \left[\sum_{i=1}^{5} d_i(age)\ x\ M_i(\lambda)\right] + d_{neutral} \qquad 4.7$$

where D_{media} is the optical density of the ocular media at wavelength λ which ranged from 380 – 780 nm, M_i is a template of one of the media components, and d_i is an age-related scaling factor for M_i. The $d_{neutral}$ is a term to account for nonselective absorption by the media and light loss due to scattering by large molecules.

The change in optical density (ΔOD_λ) between the two ages were converted into a transmittance ratio for each model by,

$$t_{R\lambda} = 10^{-\Delta OD_\lambda} \qquad 4.8$$

This ratio can also be calculated from,

$$t_{R\lambda} = \frac{t_{74,\lambda}}{t_{32,\lambda}} \qquad 4.9$$

The ratio was included in equations 4.1 - 4.3 to adjust for the change in the media transmittance that occurs between the 32-year-old and the 74-year-old by multiplying the D65 spectral power distribution by this ratio. The tristimulus values were calculated with the *Y* stimulus value for D65 normalized to 100 for each observer.

4.2.1 *Decreased Retinal Illumination*

In addition to the change in the relative spectral transmittance, there is also a decrease in the retinal illumination in the older observers. The decrease is due to pupil miosis and a decrease in the ocular media luminous transmittance. Including this reduction in the calculations is important because the CIECAM02 values are dependent on adapting luminance, L_A and this value is based on a young standard observer. Therefore, the *effective* luminance for the older observers will be less and should be included in the calculations. The next sections discuss how these light losses were estimated.

4.2.1.1 *Pupil Miosis*

Pupil diameters for the two ages were calculated using Watson and Yellot's (2012) unified formula for a light adapted visual system. Their equation is,

$$d_u = d_{SD}(F,1) + (y - y_o)[0.02132 - 0.009562 d_{SD}(F,1)] \qquad 4.10$$

The first term is the Stanley-Davies formula that relates to corneal flux and whether the scene is viewed with one or both eyes for the reference age of 28.58 yrs. This formula is,

$$d_{SD} = E\left[7.75 - 5.75\left(\frac{(La/846)^{0.41}}{(La/846)^{0.41}+2}\right)\right] \qquad 4.11$$

where L is luminance in cd/m^2 for a white light, a is the size (in deg^2) of the stimulus in a dark surround driving the pupil size, and E=1 for binocular viewing or E=0.1 for monocular viewing. The quantity La in equation 4.11 is the corneal flux density, F, and the 1.0 indicates binocular viewing.
The second term is used to adjust the pupil diameter according to age, where y is age in years, and y_o is the reference age of 28.58 years.

The calculations were done using free-ware MATLAB code written by Wheatley and Spitschan (Wheatley and Spitschan, version Oct 30, 2018).
The assumed viewing conditions were,
Luminance = 31.85 cd/m^2, which is the adapting luminance, L_A will be explained below.
Ages = 32 and 74 years respectively
Stimulus diameter, a = 20^o with binocular viewing. This size was used because the Stanley and Davies formula was evaluated to approximately 20^o. Nevertheless, we calculated beyond 20^o out to 80^o to find out the implications of extrapolating the formula to larger stimuli. Figure 4.1 shows the pupil areas as a function of stimulus size and age. The maximum difference in pupil size between the observers occurred at 2^o. The difference decreases as the stimulus size gets larger. At 20^o, the ratio of the pupil areas was approximately halfway between the ratios at these two extremes. This is another reason for selecting 20^o as the stimulus size for determining the pupil diameter. The Stiles Crawford correction is not necessary since the pupil diameters used are less than 5 mm (Sloan, 1940).

The pupil diameter of the young observer was 4.35 mm, and the diameter of the older observer was 3.46 mm. The ratio of the pupil area for the older observer to the area for the young observer is the reduction in retinal illumination due to the decrease in pupil size. That value was 0.63.

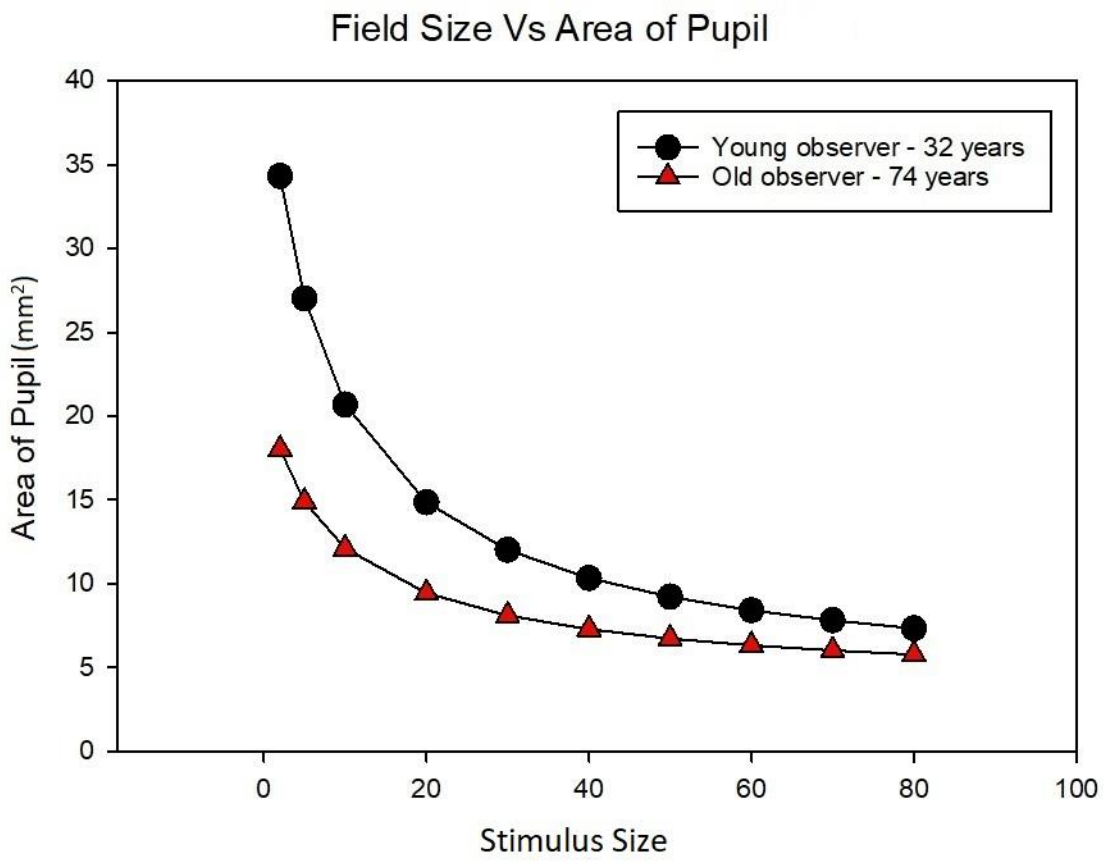

Figure 4.1: Plot of pupil size (area) at different field of view sizes for a young adult and an aged observer.

4.2.2 *Decrease in luminous transmittance*

The increase in the spectral optical density with age will also lower the luminous transmittance of the media and thus, the retinal illumination. This factor was calculated by,

$$t = \frac{\sum_{380}^{780} S_{e\lambda}\, y'_{\lambda}\, t_{R\lambda old}}{\sum_{380}^{780} S_{e\lambda}\, y'_{\lambda}} \qquad 4.12$$

where the Y value for D65 was normalized to 100 for only the younger observer and $t_{R\lambda}$ is the relative change in transmittance ratio for the old observer. This adjustment assumes that there is no change in transmittance in the longer wavelengths greater than 700 nm for the Pokorny et al. model.

The relative change in luminous transmittance from a 32-year-old to a 74-year-old for Pokorny et al.'s model was 0.75, and that for van de Kraats and van Norren's model was 0.83.

Combining the decreased pupil size and reduction in luminous transmittance results in a total reduction in retinal illumination of 0.48 for the Pokorny et al. model and 0.54 for the van de Kraats and van Norren's

model. The L_A for the older observers was multiplied by these factors to take into account the reduction in the overall retinal illumination.

4.3 Calculation of the chromaticity coordinates of FM100 Hue caps

4.3.1 *Setting of parameters*

The CIECAM02 parameters were calculated by expanding a spreadsheet provided by Dr. Fairchild's lab (available at http://markfairchild.org/CAM.html). The viewing conditions assumed for our calculations were a modified surface colour evaluation in a light booth condition (CIE, 2004). The difference from the standard light booth conditions is that we assumed an illumination level of 500 lx for a young observer, and due to the reduction in retinal illumination for the older observers, the values were 240 lx and 270 lx. The 500 lx is close to the value of commercial light sources for colour vision testing (Dain et al., 2019). Assuming an average surround condition sets the values of c and N_c. Table 4.1 lists these values.

Our input data for the CIECAM02 included the tristimulus values of the caps (XYZ), the white point ($X_wY_wZ_w$), the surround parameters, and the adapting luminance, L_A (taken to be 20% of the luminance of a white object in the scene). For the older observers, three different adaptations were examined. This allowed us to estimate how chromatic adaptation counteracts the media absorption changes in older observers. The viewing conditions with adaptation used an adaptation factor, D equal to 1.0 or 0.67. The value of D was set to 1.0 for complete adaptation and 0.67 for partial adaptation for the older observer. The choice of 0.67 was based on the recommendations of (Smet et al., 2017) that partial adaptation provided a better fit to colour appearance for yellowish lights for young observers. D was set to zero for the no adaptation condition for the older observers. Table 4.2 lists the CIECAM02 variables that were set by the viewing conditions or calculated for the respective observers and adaptation condition but were constant across caps for that observer and adaptation condition (CIE, 2020b).

Table 4.1: Parameter settings for surface colour evaluation in a light booth

Example	**Ambient lighting in lx (cd/m^2)**	**Scene or device white luminance**	**Adapting luminance, L_A in cd/m^2**	**Adopted white point**	**Surround ratio, S_R (L_{SW}/L_{DW})**	**Surround**
Surface colour evaluation in a light booth: Young	500 (159.15)	159.15 cd/m^2	31.85	Light booth WP X_w= 95.04 Y_w=100.00 Z_w= 108.84	0.20	Average N_c = 1.00 c = 0.69
Surface colour evaluation in a light booth: Old Observer (Pokorny et al.)	500 (159.15)	159.15 cd/m^2	15.45	X_w= 47.29 Y_w= 48.49 Z_w= 27.09		Average N_c = 1.00 c = 0.69
Surface colour evaluation in a light booth: Old observer (van de Kraats and van Norren)	500 (159.15)	159.15 cd/m^2	17.12	X_w= 49.67 Y_w= 53.76 Z_w= 29.68		Average N_c = 1.00 c = 0.69

4.3.2 *CIECAM02 parameters under different conditions of adaptation*

Tables 4.3a, 4.3b, and 4.3c show the list of parameters used for our calculation for the young and old observers under different conditions of adaptation. Major differences between the young and old observers were found in the adapting luminance, L_A and its related parameters such as the luminance-level adaptation factor, F_L, background luminance factor, n, brightness, and background induction factors, N_{bb}, N_{cb}.

Table 4.2a: Summary of CIECAM02 parameters – with adaptation

CAM02 Parameter	Young	Old - van de Kraats	Old – Pokorny
Degree of adaptation, ***D***	1.00	1.00	1.00
Adapting luminance, L_A *(cd/m*^{2}*)*	31.85	17.12	15.45
Maximum degree of adaptation, ***F***	1.00	1.00	1.00
Background relative luminance, Y_b	20.0	20.0	20.0
Exponential nonlinearity, ***c***	0.69	0.69	0.69
Chromatic induction factor, N_c	1.00	1.00	1.00
Viewing condition constant, ***k***	0.006	0.012	0.013
Luminance-level adaptation factor, F_L	0.54	0.44	0.43
Background luminance factor, ***n***	0.20	0.37	0.37
Brightness induction factor, N_{bb}	1.00	0.88	0.87
Background induction factor, N_{cb}	1.00	0.88	0.87
Base exponential nonlinearity, ***z***	1.93	2.09	2.12

Table 4.2b: Summary of CIECAM02 parameters – with partial adaptation

CAM02 Parameter	Young	Old - van de Kraats	Old – Pokorny
Degree of adaptation, ***D***	1.00	0.67	0.67
Adapting luminance, L_A *(cd/m2)*	31.85	17.12	15.45
Maximum degree of adaptation, ***F***	1.00	0.79	0.79
Background relative luminance, Y_b	20.0	20.0	20.0
Exponential nonlinearity, ***c***	0.69	0.69	0.69
Chromatic induction factor, N_c	1.00	1.00	1.00
Viewing condition constant, ***k***	0.006	0.012	0.013
Luminance-level adaptation factor, F_L	0.54	0.44	0.43
Background luminance factor, ***n***	0.20	0.37	0.37
Brightness induction factor, N_{bb}	1.00	0.88	0.87
Background induction factor, N_{cb}	1.00	0.88	0.87
Base exponential nonlinearity, ***z***	1.93	2.09	2.12

Table 4.2c: Summary of CIECAM02 parameters and TES – without adaptation

CAM02 Parameter	Young	Old - van de Kraats	Old – Pokorny
Degree of adaptation, ***D***	1.00	0.0	0.0
Adapting luminance, L_A *(cd/m²)*	31.85	17.12	15.45
Maximum degree of adaptation, ***F***	1.00	0.0	0.0
Background relative luminance, Y_b	20.0	20.0	20.0
Exponential nonlinearity, ***c***	0.69	0.69	0.69
Chromatic induction factor, N_c	1.00	1.00	1.00
Viewing condition constant, ***k***	0.006	0.012	0.013
Luminance-level adaptation factor, F_L	0.54	0.44	0.43
Background luminance factor, ***n***	0.20	0.37	0.37
Brightness induction factor, N_{bb}	1.00	0.88	0.87
Background induction factor, N_{cb}	1.00	0.88	0.87
Base exponential nonlinearity, ***z***	1.93	2.09	2.12

4.3.3 *Colour differences between caps and predicted arrangements*

The colour difference between adjacent caps was calculated using the CIECAM02 – SCD (small colour differences) equations (Luo et al., 2006). The equations are,

$$\Delta E = \sqrt{(\Delta J'/K_L)^2 + \Delta a_M^2 + \Delta b_M^2} \qquad 4.19$$

$$\text{where } J' = (1 + 100c_1)J/1 + 100c_1J \qquad 4.20$$

$$M' = (1/c_2)\ln(1 + c_2 M) \qquad 4.21$$

$$a_M = M'\cos(h) \qquad 4.22$$

$$b_M = M'\sin(h) \qquad 4.23$$

where *J′, M′, h* are CIECAM02 lightness, colourfulness, and hue angle values respectively. The values a_M and b_M are chromaticity coordinates (Luo et al., 2006). The terms $\Delta J'$, Δa_M and Δb_M are the differences in the *J′,* a_M and b_M between the FM100 Hue caps. The K_L, c_1, and c_2 are coefficients whose values are dependent on the CAM02 type, i.e., CAM02-LCD, CAM02-SCD, and CAM02-UCS (Table 4.4).

Table 4.4: The coefficients of modified CAM02 model (Luo et al., 2006)

	CAM02-LCD	CAM02-SCD	CAM02-UCS
K_L	0.77	1.24	1.00
c_1	0.007	0.007	0.007
c_2	0.0053	0.0363	0.0228

The colour difference for each cap was calculated between itself and the immediate adjacent cap, ΔE_1, between itself and the next cap in order, ΔE_2, and between itself and the third cap away in order, ΔE_3. The colour differences were entered into a grid for determining the order of the caps. The cap with the smallest colour difference was placed next to the cap under consideration. That cap then became the cap under consideration. A transposition occurred if ΔE_2 or $\Delta E_3 < \Delta E_1$ for a cap. For example, if $\Delta E_2 < \Delta E_1$ for cap 44, then cap 46 would follow after 44. For cap 46, the ΔE_1 of cap 46 would be between 46 and 45, with ΔE_2 between 46 and 47 and ΔE_3 between 46 and 48. The cap with the smallest ΔE would follow cap 46. This process was repeated to predict the ordering of the caps under each condition of adaptation. The total error score (TES) of each predicted arrangement was calculated using the method that includes the anchor caps using an Excel spreadsheet version 2106 (Kinnear and Sahraie, 2002). The partial error scores for red-green (RG) and blue-yellow (BY) were also calculated (Smith et al., 1985). The mean color difference between adjacent caps was also calculated based on the tray and whether they were in one of the red-green or blue-yellow quadrants caps.

Chapter 5

Results

5.1 Introduction to the chapter

This chapter presents the predicted order of the FM100 for an ideal young and older adult observer. The media transmittance for the older observer was modeled using van de Kraats and van Norren and Pokorny et al. media transmittance models.

5.2.1 *Standard viewing conditions with complete adaptation*

Table 5.1 lists the different parameters used in the CIECAM02 with complete adaptation (D = 1). Figure 5.1 shows the chromaticity coordinates of the caps for the 3 observers. The size of the gamut (i.e., size of the area in the chromaticity space enclosed by the caps' coordinates) for the older observers was slightly smaller than the young observer, indicating that most caps appeared less saturated to the older observer. Figures 5.2 and 5.3 show the FM100 error plots for the predicted ordering of the young observer and the two older observers. The errors for all 3 observers occurred in the lower portion of the plot, which corresponds to trays 3 and 4. The arrangements of all 3 observers show errors at caps 44 - 47 and 61 - 64. The older observers have an increase in transpositions for caps 56-59. The arrangements for the two older observers were identical. The total error score (TES) for the young observer was 8, with a partial red-green (RG) and blue-yellow (BY) error score of 4 each. For both older observer models, the TES was 12, with an RG error score of 8 and BY error score of 4.

Table 5.1: CIECAM02 parameters with adaptation

CAM02 Parameter	Young	Old - van de Kraats	Old - Pokorny
D	1.00	1.00	1.00
L_A (cd/m^2)	31.85	17.12	15.45
F	1.00	1.00	1.00
Y_b	20.0	20.0	20.0
c	0.69	0.69	0.69
N_c	1.00	1.00	1.00
k	0.006	0.012	0.013
F_L	0.54	0.44	0.43
n	0.20	0.37	0.37
N_{bb}	1.00	0.88	0.87
N_{cb}	1.00	0.88	0.87
z	1.93	2.09	2.12

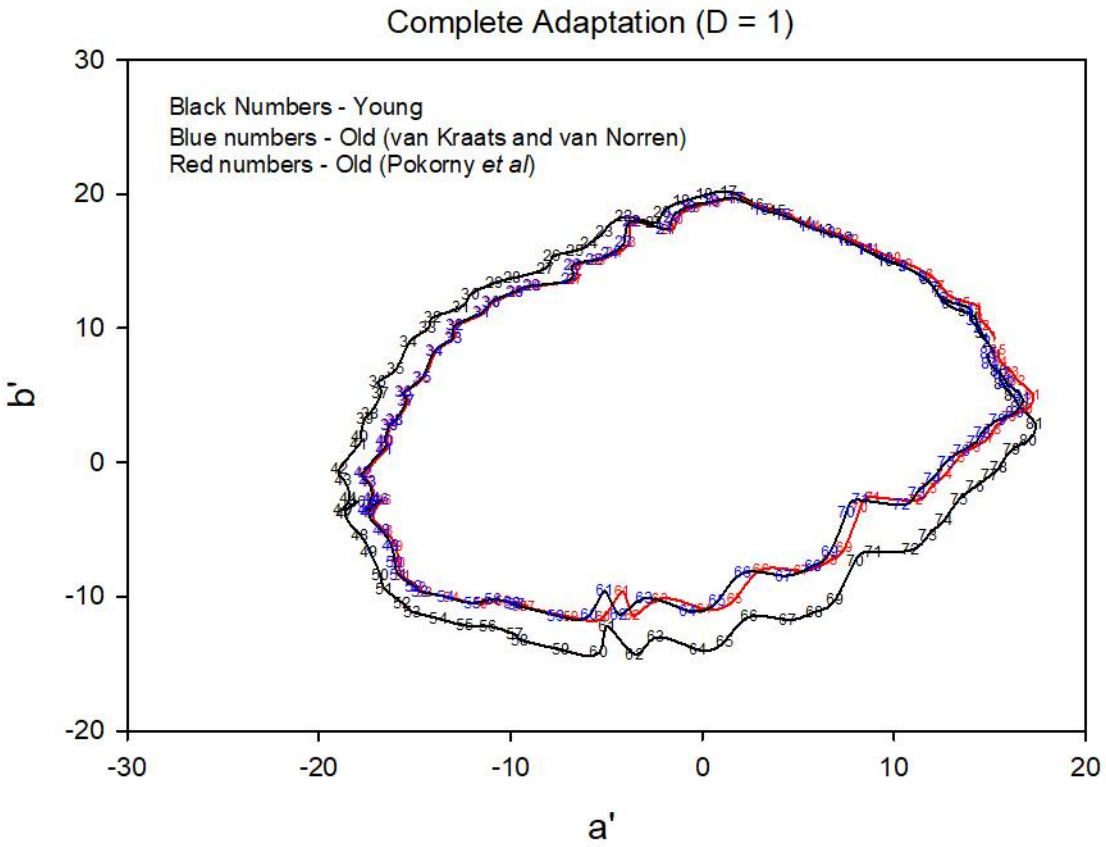

Figure 5.1: Chromaticity coordinates of the FM100 hue caps in the CIECAM02 a' b' diagram for the 3 observers. The numbers correspond to the cap numbers.

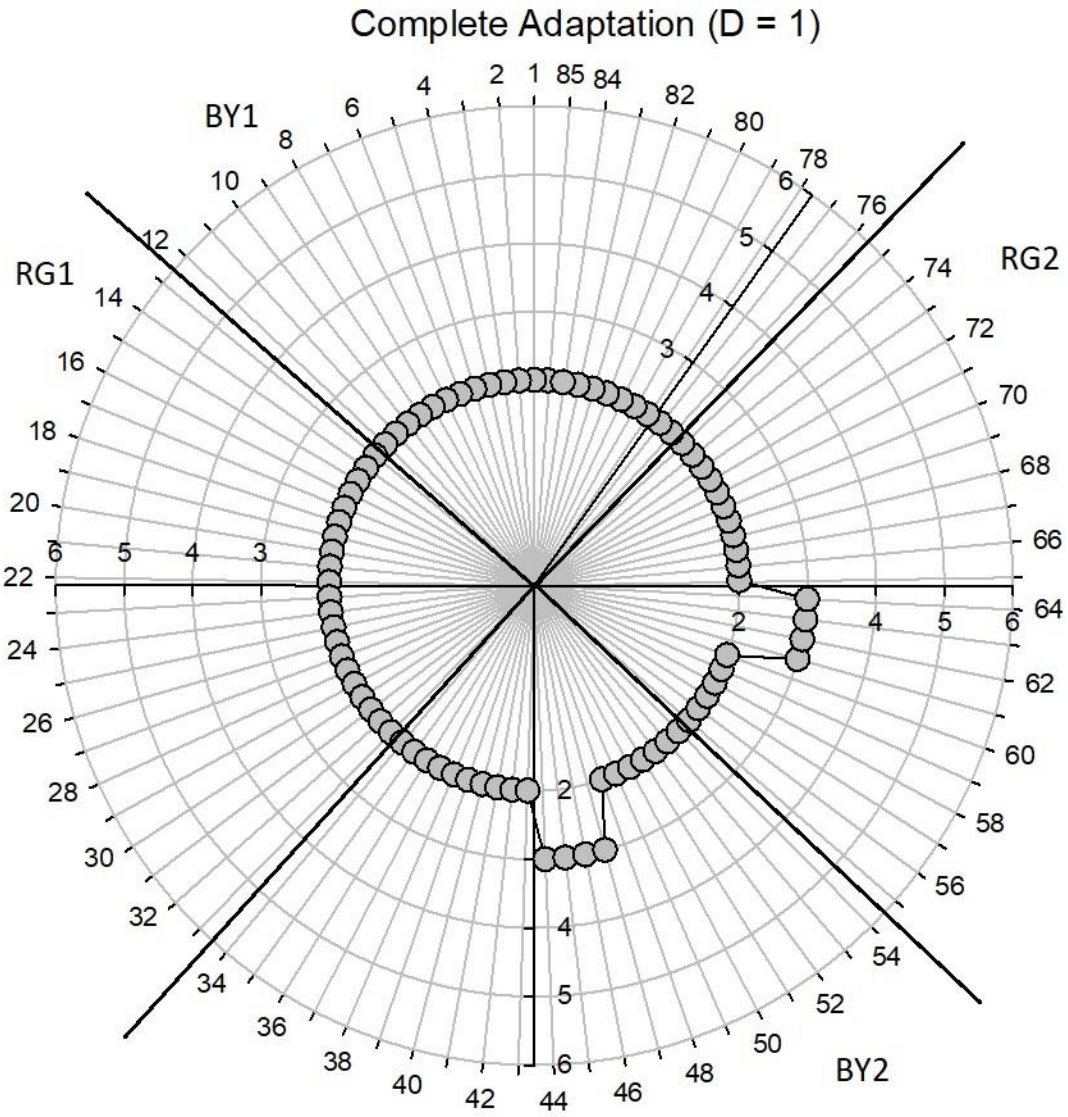

Figure 5.2: Predicted cap error scores for the young observer under complete and partial adaptation. A score of 2 indicates that the two adjacent caps were in the correct order. A score of 2 indicates the correct arrangement of the two adjacent caps.

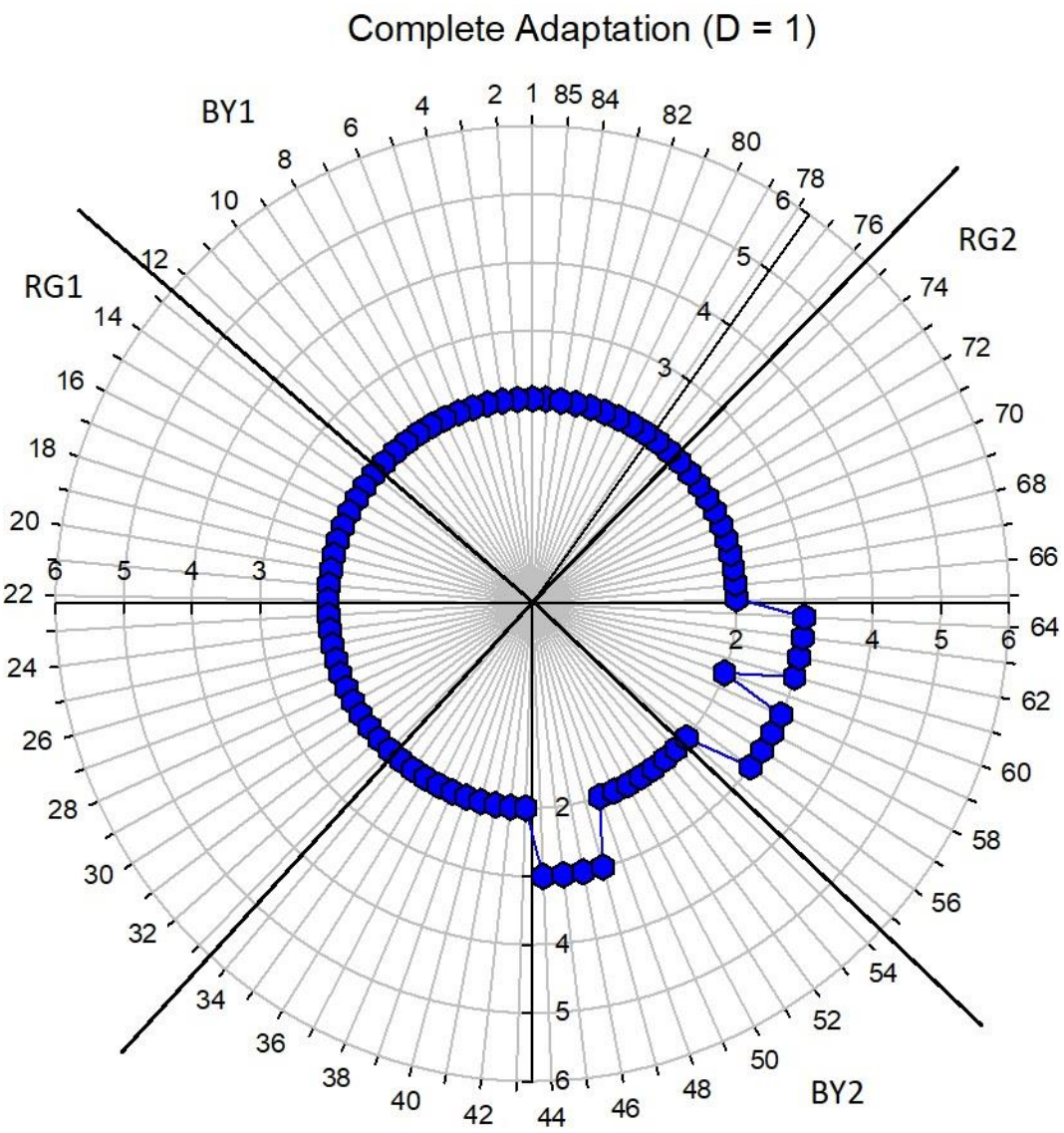

Figure 5.3: Predicted cap error scores for the old observers under complete and partial adaptation. The order was identical for both older observer models. A score of 2 indicates the correct arrangement of the two adjacent caps.

5.2.2 *Partial adaptation factor*

Figure 5.4 shows the chromaticity coordinates for the adaptation factor, D = 0.67. The chromaticity coordinates of the individual caps were similar for the two older observers, but the size of their gamut was appreciably smaller than the young adult. Although the gamut size was smaller, the ordering and, consequently, the error scores were identical to the results with complete adaptation condition.

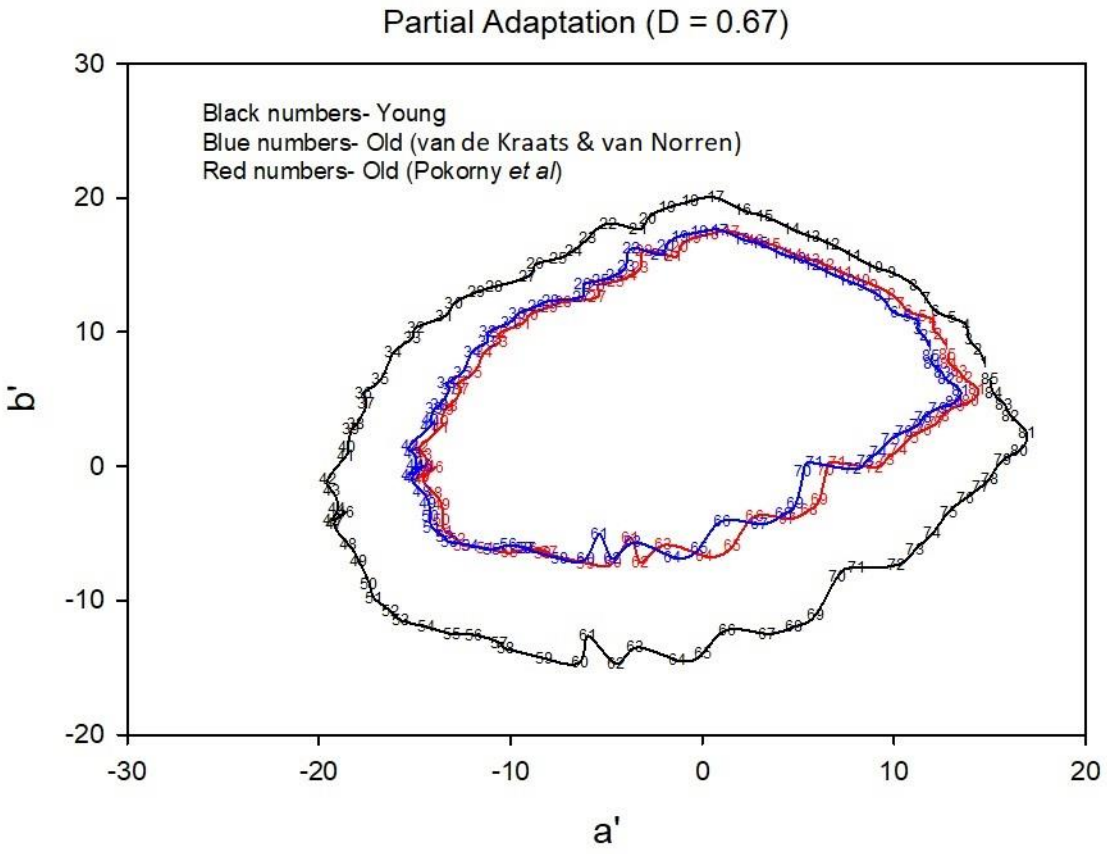

Figure 5.4: Chromaticity coordinates of the FM100 hue caps in the CIECAM02 a' b' diagram for the 3 observers when the adaptation factor was D = 0.67.

5.2.3 *No adaptation*

Figure 5.5 shows the chromaticity coordinates of the FM100 without any adaptation occurring for the older observers. The gamut for the older observers was vertically shifted towards yellow from the gamut of the young adult and decreased in size. Thus, there is a change in both hue and chroma for the older observers. The error scores of both older observers increased relative to the adapted states, but the increase was similar for both older observer models. The van de Kraats and van Norren observer had a TES of 16, with an RG score of 12 and BY score of 4. The Pokorny et al. observer had a slightly higher TES of 20, with an RG score of 12 and BY score of 8. The cap transpositions for each observer are illustrated by the polar plots (Figures 5.6 and 5.7). The difference between the two aged observers was in the arrangements for caps 44 to 48, in tray 3.

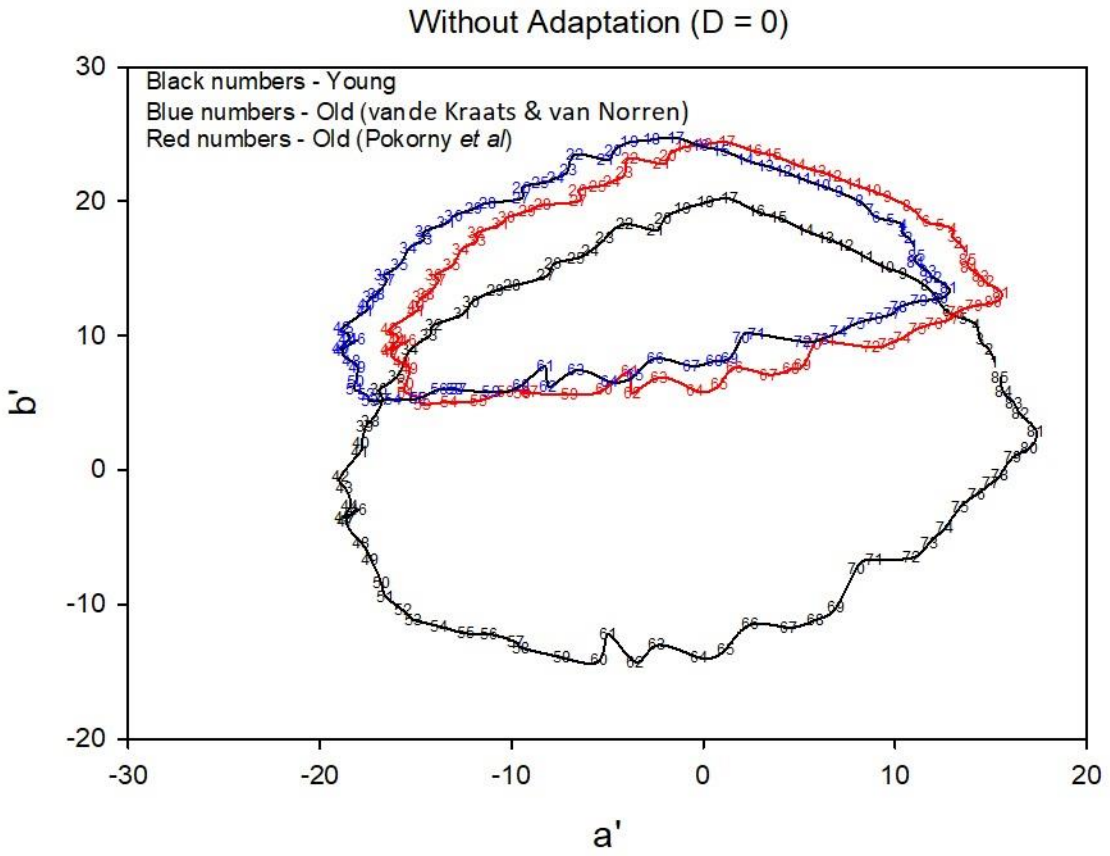

Figure 5.5: Chromaticity coordinates of the FM100 hue caps in the CIECAM02 a' b' diagram for the 3 observers when the adaptation factor, D, was reduced to zero for the older observers.

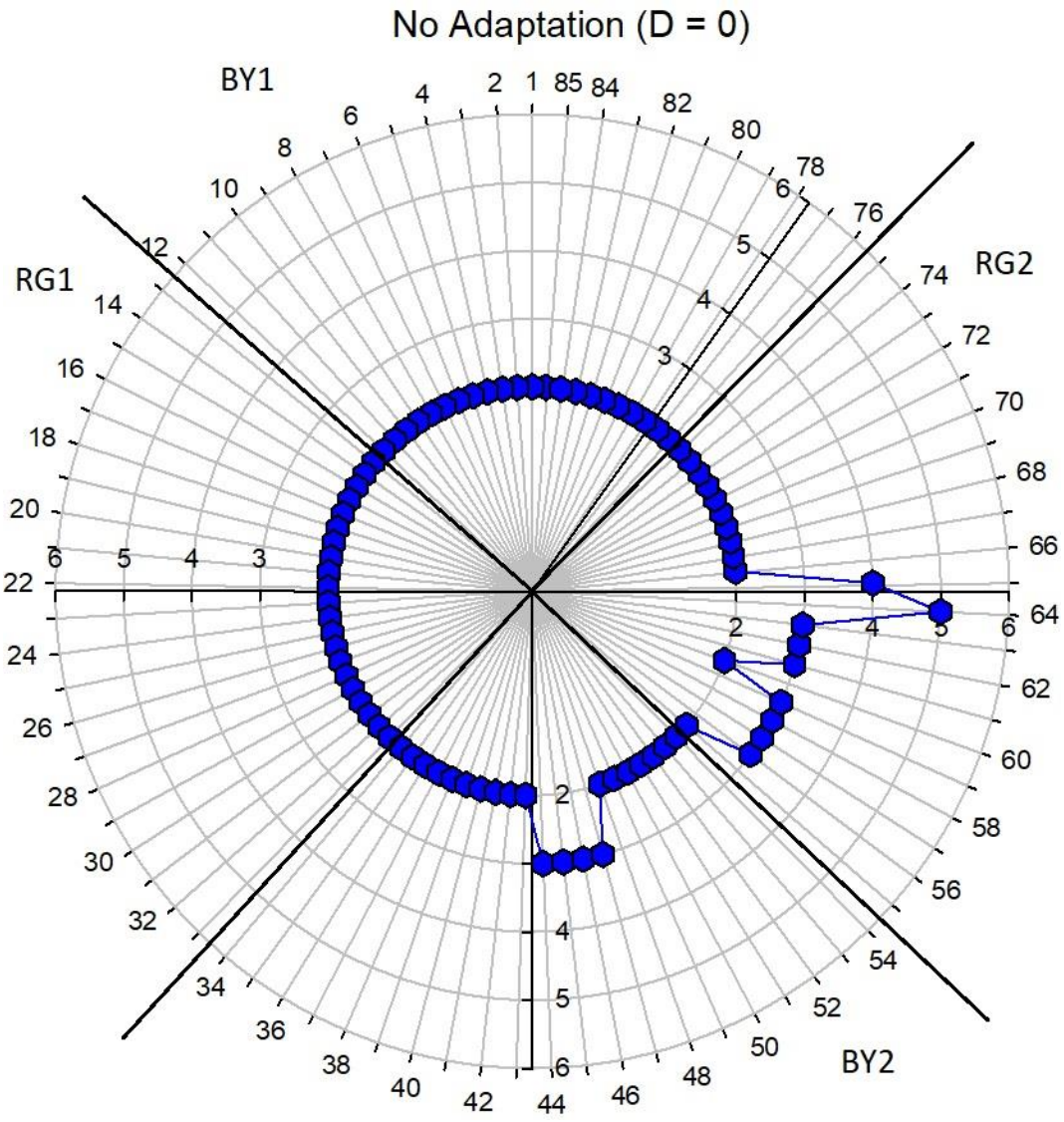

Figure 5.6: Predicted cap error scores for the van de Kraats and van Norren old observer with no adaptation. A score of 2 indicates that the two adjacent caps were in the correct order.

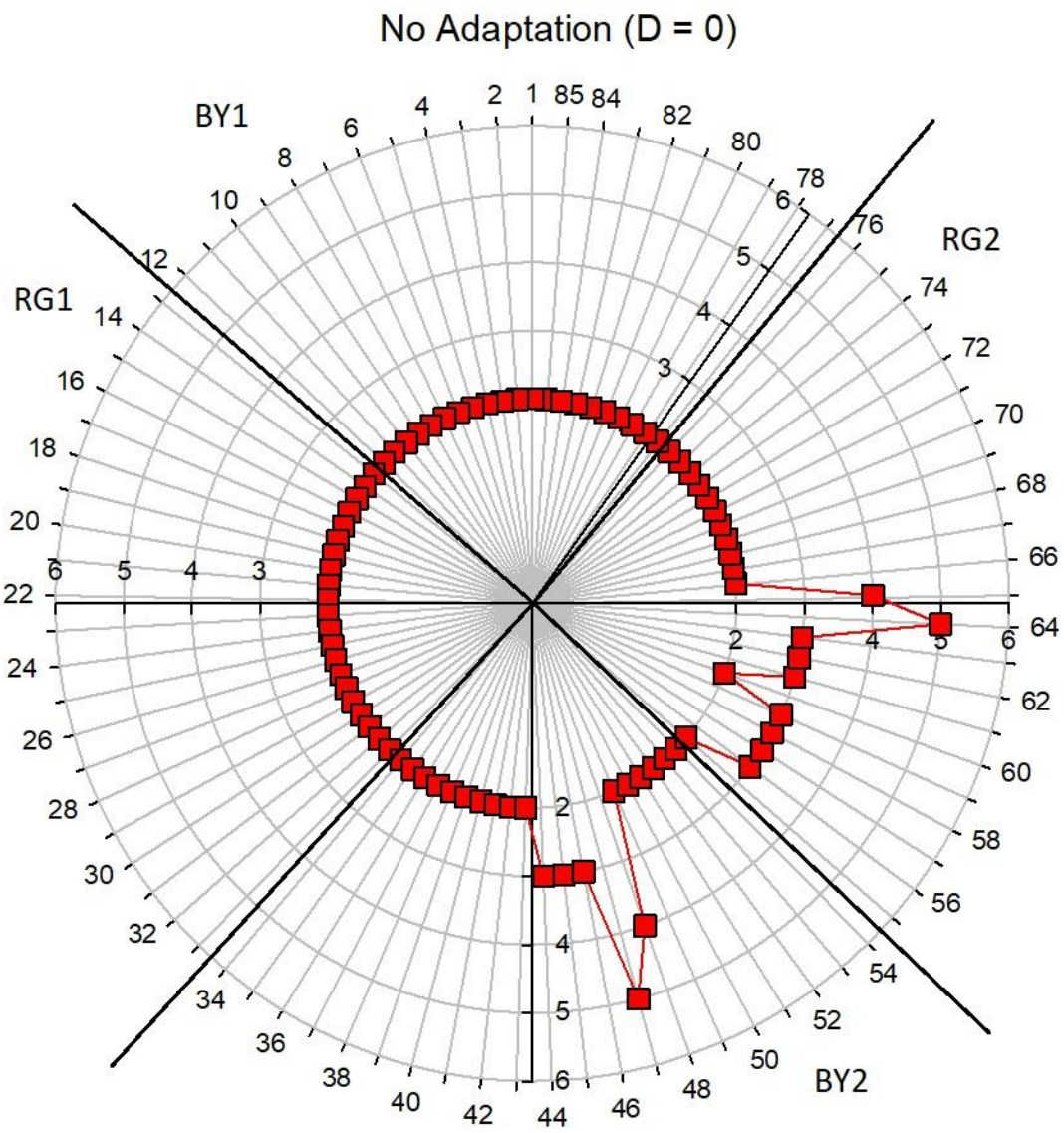

Figure 5.7: Predicted cap error scores for the Pokorny et al. old observer with no adaptation. A score of 2 indicates that the two adjacent caps were in the correct order.

5.3 Comparison of colour differences

A reduction in the gamut area for the two conditions where adaptation was not complete indicates that the colours would appear less saturated, and the difference between the colours of adjacent caps could be smaller. We calculated the mean and standard deviations of color differences between adjacent caps for each condition and observer to quantify this latter change. The groups were organized by tray and the RG and BY quadrants.

5.3.1 *Complete adaptation*

Figure 5.8 shows that the mean colour differences for the young observer were slightly larger than the two older observers. However, the tray means and standard deviations for the older observers were nearly identical. The exception was tray 3, where the Pokorny et al. observer had marginally higher values than the van de Kraats and van Norren observer. Figure 5.9 shows that the mean colour difference when partitioned into BY and RG quadrants. Although the mean values are very similar based on the standard deviations, the colour differences for the blue-yellow quadrants were smaller than the differences for the red-green caps for all observers, but the difference between the BY and RG colour differences was slightly larger for the older observers. The difference between the Pokorny et al. and van de Kraats and van Norren models is not as obvious because tray 3 is divided between the BY2 and RG2 quadrants and that division obscures the difference between the models shown in Figure 5.8.

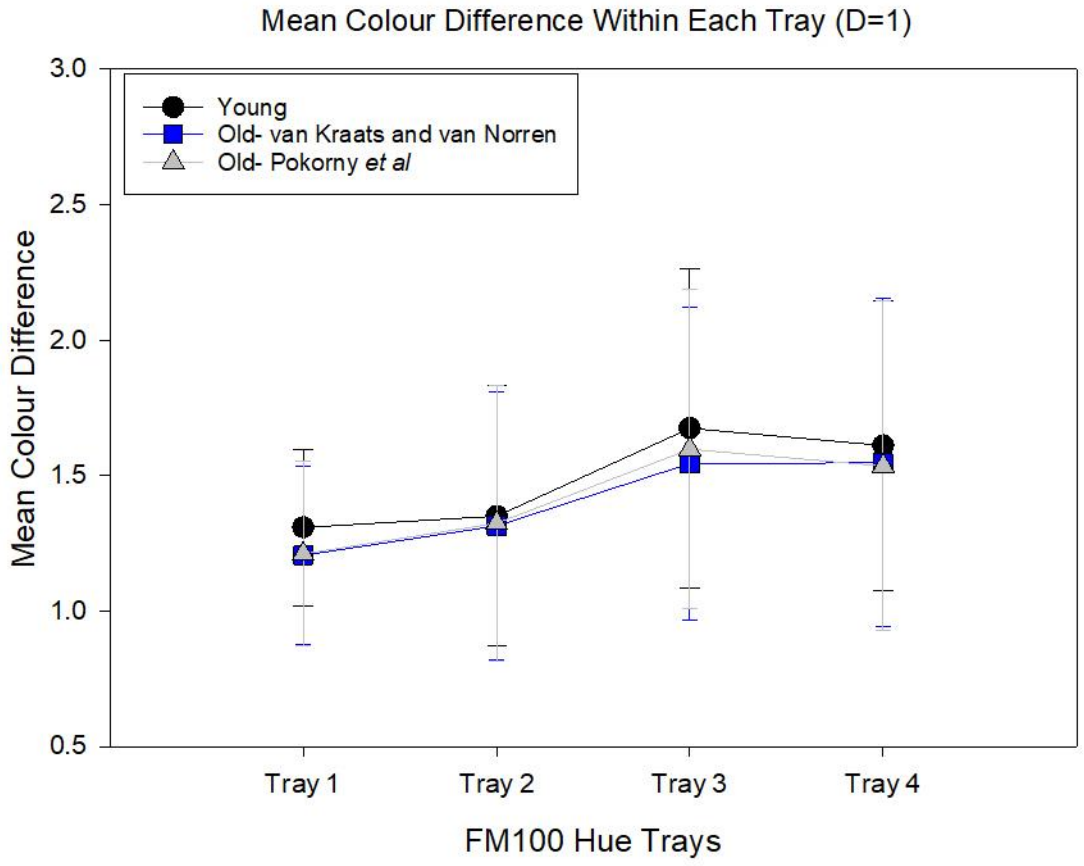

Figure 5.8: Mean colour difference between adjacent caps in the CIECAM02 chromaticity space for each tray and observer with complete adaptation. Error bars are the standard deviations.

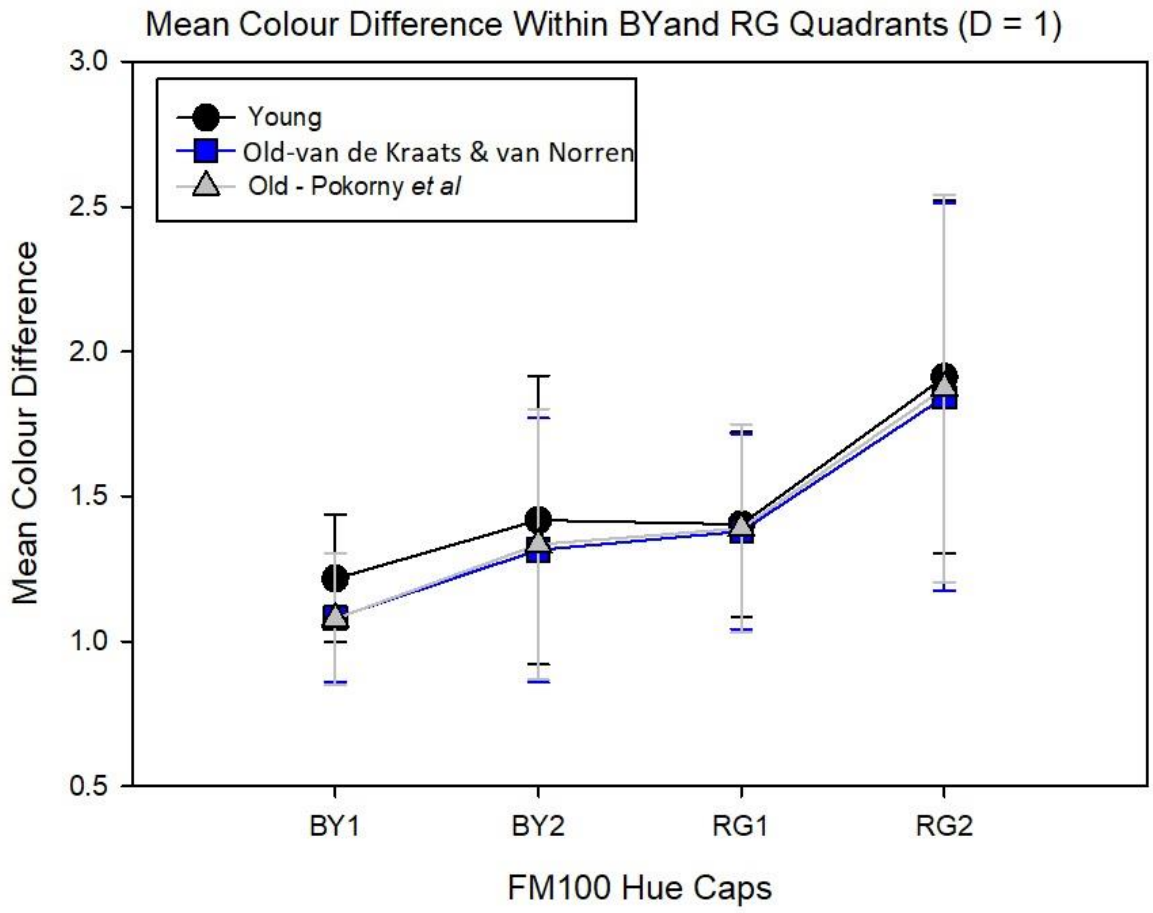

Figure 5.9: Mean colour difference between adjacent caps in the CIECAM02 chromaticity space along BY and RG axis for each observer with complete adaptation. Error bars are the standard deviations.

5.3.2 *Partial adaptation*

Figure 5.10 shows mean differences for the young and the old observers with partial adaptation for older observers (D = 0.67). The difference between trays and observers were similar to the results with complete adaptation. Figure 5.11 also shows the mean differences for the observers partitioned within the BY and RG quadrants. The observed pattern is similar to the mean colour difference under complete adaptation even though there were marginal differences.

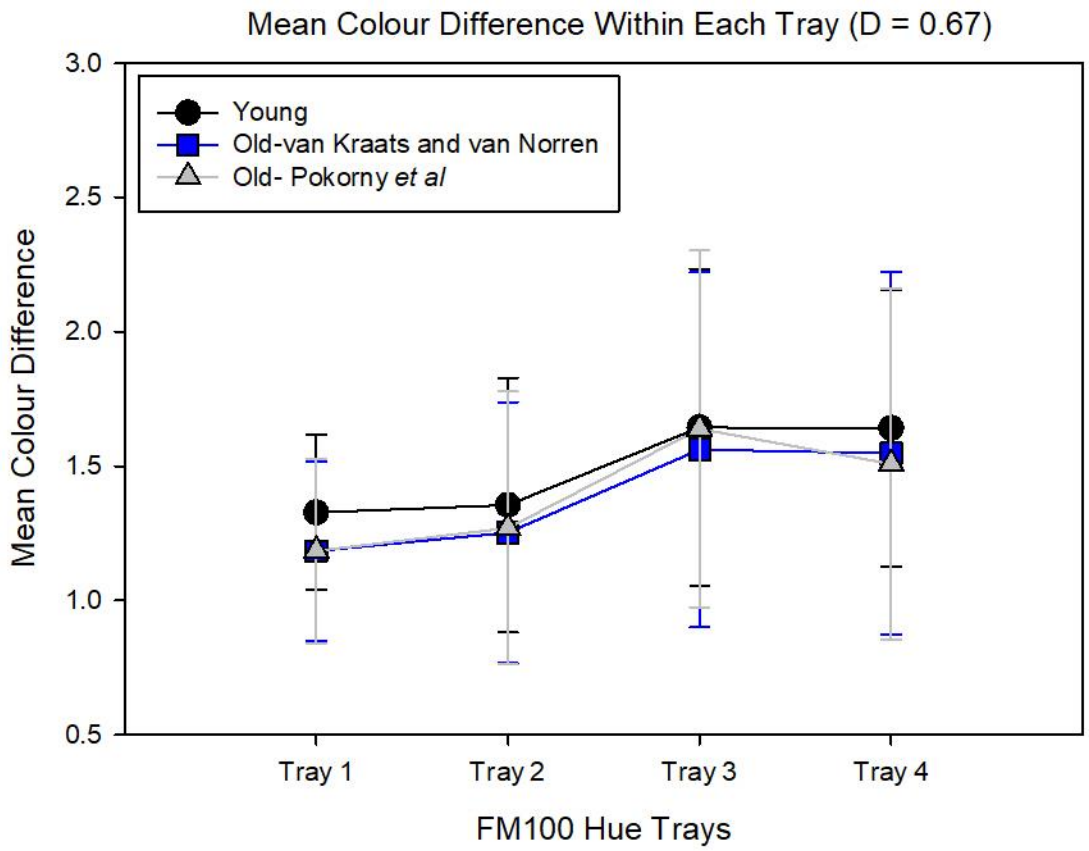

Figure 5.10: Mean colour difference between adjacent caps in the CIECAM02 chromaticity space for each tray and observer with partial adaptation. Error bars are the standard deviations.

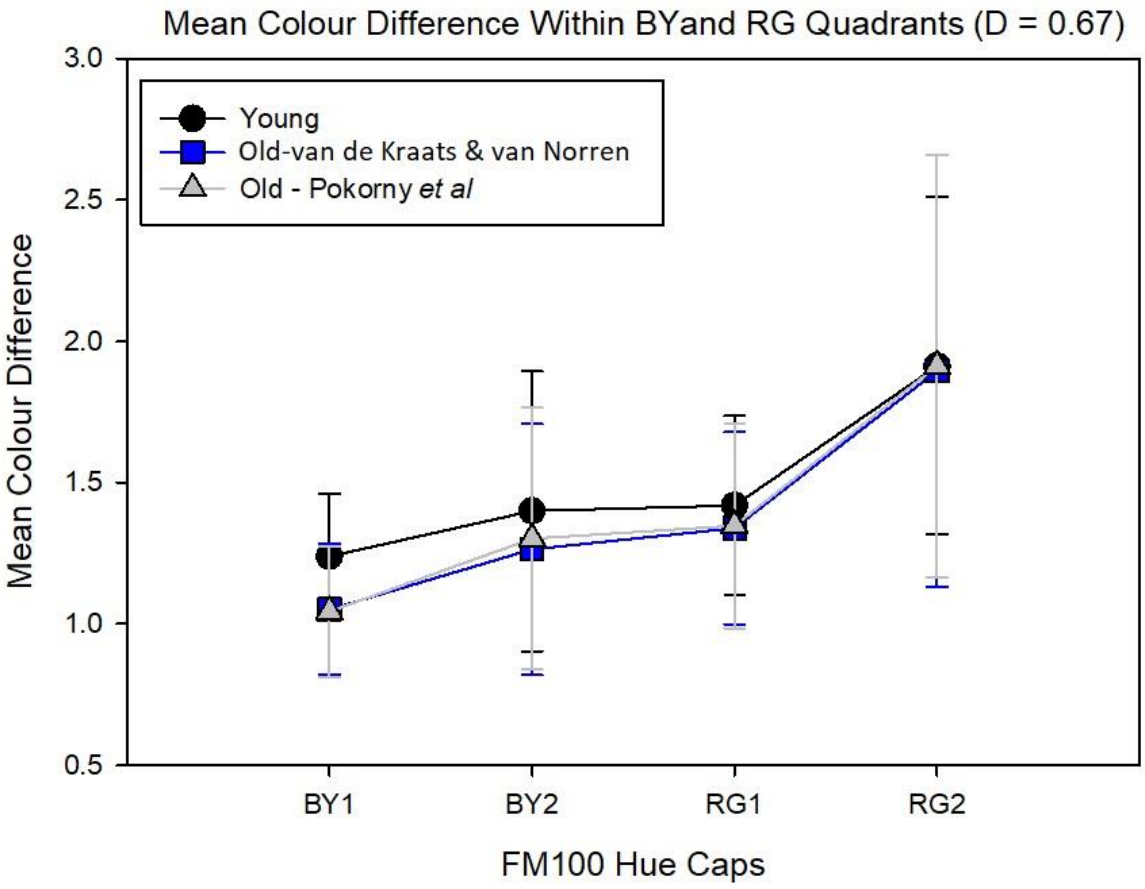

Figure 5.11: Mean colour difference between adjacent caps in the CIECAM02 chromaticity space along BY and RG axis for each observer with partial adaptation. Error bars are the standard deviations.

5.3.3 *No adaptation*

Figure 5.12 shows the colour differences without chromatic adaptation for the older observers. The means of the older observers were uniformly lower than with complete adaptation and was highest in tray 3. Figure 5.13 shows a similar pattern for the RG and BY error scores where there is also a uniform reduction in colour differences for the older observers. The colour differences between the models for tray 3 are present and are relatively larger than for the adaptation condition. The no adaptation condition's larger colour differences between models are due to the smaller mean value for the van de Kraats and van Norren colour differences. The smaller colour differences in tray 3 for the van de Kraats and van Norren model are also reflected in the mean colour differences in the BY2 quadrant.

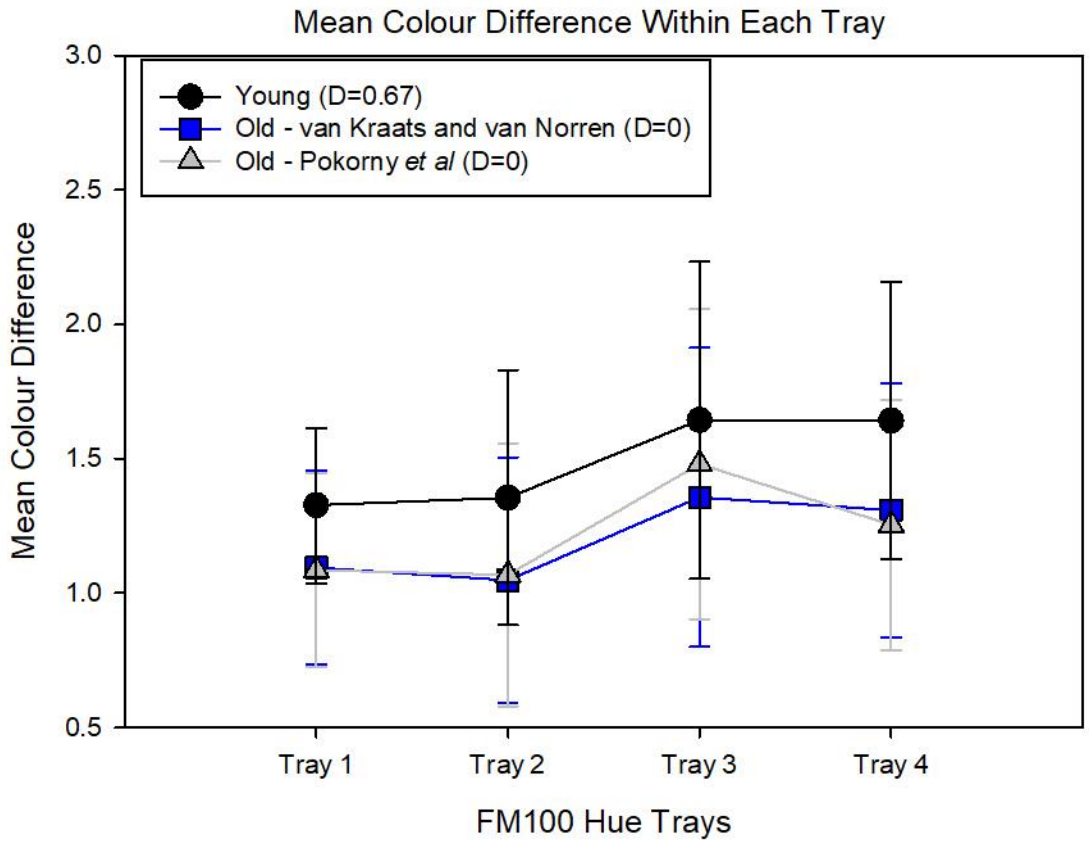

Figure 5.12: Mean colour difference between adjacent caps in the CIECAM02 chromaticity space for each tray and observer with partial adaptation for the young observers and without adaptation for the older observers. Error bars are the standard deviations.

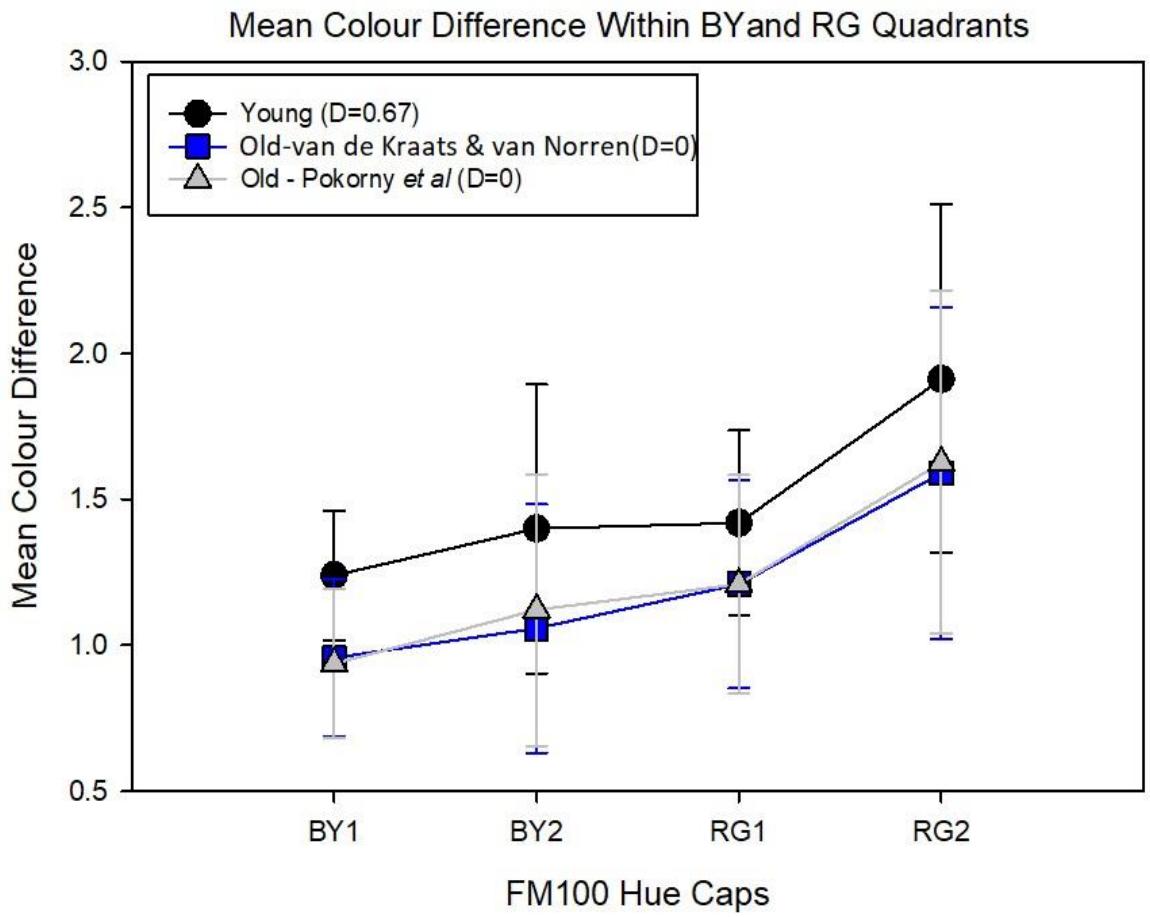

Figure 5.13: Mean colour differences between adjacent caps in the CIECAM02 chromaticity space along BY and RG axis with partial adaptation for the young observers and without adaptation for the older observers. Error bars are the standard deviations.

5.4 Conclusion to the chapter

We found that the older models with or without adaptation had a different ordering pattern from the young. The errors for the younger observer were in trays 3 and 4, which resulted in equal RG and BY partial error scores. With complete and partial adaptation in both models of the older eye, there was increase in the TES due to an increase in errors in the RG2 quadrant (i.e., tray 3). Without adaptation, the error score increased further for the older observer models. Both older observer models had additional errors for caps 55 to 66 in the RG2 quadrant. The Pokorny et al observer had additional errors for caps 44 to 48 in the BY2 quadrant. The colour difference between adjacent caps was slightly reduced for the older observers in the BY quadrants, but not the red-green quadrants if complete or partial adaptation occurred. Without adaptation, the colour difference between the BY caps decreased slightly more, whereas there was a larger decrease in the mean colour difference for the RG caps.

Chapter 6

Discussion and Conclusion

6.1 Introduction to the chapter

The results showed how changes in the media transmittance with age, particularly the crystalline lens, can affect the FM100 cap arrangements. One of the questions surrounding this issue is the effect of chromatic adaptation on the FM100 Hue caps ordering. The CIECAM02 is one colour specification system that allows us to examine that question. In this thesis, we assume that the other neural processes are unaffected by age except for the adaptation mechanism. This chapter presents the discussion of FM100 hue test for our model observers.

6.2 Total error score and chromatic discrimination

Based on the cap's chromaticity coordinates under the standard Illuminant D65, the ideal young, 32-year-old observer was not perfect, but the errors were minimal. Relative to previous psychophysical studies, the young observer's error score (8) was consistent with the minimum error scores for the 30-34 years of Verriest (1963) study. Our predicted error score was also 1.7 – 2 standard deviations better than the mean error scores of the studies of Verriest (1982) and of Mantyjarvi (2001). The transpositions were equally distributed along the red-green and blue-yellow axis but were confined to trays 3 and 4.

Our findings that errors occurred in tray 3 and no errors occurred in tray 1 are in line with Lakowski's colorimetric evaluation of the FM100 Hue test. Based on the average colour difference between adjacent caps in his study, arranging the caps in tray 3 should be the most difficult, followed by trays 2, 4, and 1 (Lakowski, 1966). Our predicted results that errors occurred in trays 3 and 4, but not in trays 1 and 2 were closer in agreement with Mantyjarvi's (2001) psychophysical data that the error score was highest for tray 4, followed closely by tray 3, tray 2, and then tray 1. The difference in Mantyjarvi's results and our predictions from Lakowksi's colorimetric findings could be due to variability in the different production run of the FM100 Hue test and in equipment used to measure the cap reflectances. The different versions can alter the positions of the caps that are off the average hue circle formed by the FM100. For example, in Figure 5.1, cap 61 is displaced from the average hue circle resulting in the order of 61-63-62. If this displacement is not present in other versions, there may be no transpositions among caps 61 to 64.

The predictions for the older observers with complete and partial adaptation showed an increase in the total error score. Previous studies showed that the mean square root of the total error score increased by a factor of about 1.7 between observers aged 32 and 74 years old (Smith et al., 1985; Roy et al., 1991; Kinnear and

Sahraie, 2002). This increase in error score came quite close to the factor of 1.6 found in this study. However, the increase in the total error score in our study was in the red-green partial score and not the blue-yellow score for both models. All other psychophysical studies showed that the reduction in hue discrimination is larger along the blue-yellow axis compared with the red-green axis (Verriest, 1963; Roy et al., 1991; Mantyjarvi, 2001; Kinnear and Sahraie, 2002). For example, the square root of the blue-yellow error score increases by a factor of about 2.1 between 30 and 70 years, whereas the square root of the red-green increases by about 1.7 (Kinnear and Sahraie, 2002; Beirne et al., 2008). Similarly, Barbur and Rodriguez-Carmona's results for the Colour Assessment and Diagnosis (CAD) test suggest that the red-green error score should increase by a factor 1.5 between the ages of 32 and 74 years, and the blue-yellow should increase by a factor 1.9 (Barbur and Rodriguez-Carmona, 2015). The discrepancy of where the predicted errors should occur, and the psychophysical data indicate that reduction in hue discrimination with age is also due to age-related changes in the neural processes.

This conclusion is consistent with Lakowski's (1962) results for hue discrimination of aphakes. Based on anomaloscope colour matching data, he concluded that loss of discrimination with age resulted from other age-related changes and not only lens yellowing since the hue discrimination of aphakes was still worse than that of young adults. Mantyjarvi and Tuppurainen (1996) also reported that error scores on the FM100 Hue test in pseudophakes were not statistically different from age-matched controls. In a subsequent study, Mäntyjärvi et al. (1997) reported similar results that the FM100 Hue scores were not significantly different between pseudophakes and age-matched controls. However, they reported that error scores in tray 4 were statistically lower in the pseudophakic group. Our predictions suggest that removing the older lens should lower the error score in tray 3 for both adaptation states. Nevertheless, if adaptation does not occur as one ages, then our predictions suggest that the error score following cataract extraction could also improve. This discrepancy is another indication that age-related colour vision changes are due to both neural and media changes. Additional support indicating that neural changes are a major factor in the loss of colour discrimination with age is that the FM100 Hue error scores were similar for subjects with the clear Acrysof and yellow Acrysof Natural intraocular lens (IOL) implants; however, both pseudophakic groups had higher scores than phakic young adults (Cionni and Tsai, 2006; Vuori and Mäntyjärvi, 2006).

Ruddock (1965) concluded that age-related changes in colour vision could be attributed to selective absorption of the media and the smaller pupil. His conclusion was primarily based on colour matching and spectral sensitivity data. His results were in agreement with others who had subjects perform colour matches using an anomaloscope (Lakowski, 1962; Mäntyjärvi and Tuppurainen, 1996; Mäntyjärvi et al., 1997).

These results suggest media changes primarily produce age-related differences in the mean colour match settings and that neural changes primarily affect discrimination.

The effect of pupil miosis is more complex. If the effect of pupil miosis was just a reduction of retinal illumination, then hue discrimination should improve with increased light levels. Although the error scores do improve with increased illumination on the test, Knoblauch et al. (1987) found that the performance of the older group (70-79 years) at the maximum illumination of 1800 lx was similar to the young adults at 5.7 lx. Furthermore, the error remained predominantly along the blue-yellow axis (Knoblauch et al., 1987). Because the older observers were phakic, selective media absorption could have contributed to the residual errors, but our results suggest that the residual error should have shifted equally between red-green and blue-yellow errors if media were clear. Although the CIECAM02 does allow one to consider changes in retinal illumination, a reduction of a factor of 0.63 for the young adult did not increase the number of transpositions, and there was only a marginal decrease in both the red-green and blue-yellow mean colour differences. Because the blue-yellow colour differences were already smaller than the red-green mean colour differences, it is possible that the blue-yellow errors could increase for a non-ideal observer.

One of the questions raised by Ruddock (1965) is the role adaptation play in age-related media changes with respect to the FM100 Hue test. Our results indicate that a von Kries type of adaptation would reduce the errors but not return the score to a young adult. The result that Beirne et al. (2008) found no change in the FM100 Hue score when young adults wore filters simulating the lens transmittance of the older adult suggests that adaptation mechanisms are in place in young adults and adequate to compensate for media changes. Also, the scores of the subjects in the Cionni and Tsai (2006) study who had clear IOLs did not change when they viewed the test through yellow filters simulating the Natural IOL. This result suggests that a similar chromatic adaptation is functioning adequately in older adults. Whether this is just a von Kries adaptation mechanism or more mechanisms are involved is uncertain.

Although both models for the older observers predicted an increase in the TES, the results were slightly different between the two models. Both the van de Kraats and van Norren and Pokorny et al. models had identical predictions in the FM100 Hue results with complete or partial adaptation. With no adaptation, both models also predicted the same increase in the red-green error score; however, the Pokorny et al. model also predicted an increase in the blue-yellow error score, whereas the van de Kraats and van Norren model did not predict this increase. The difference could be due to relatively higher optical density between 450 nm and 570 nm in the Pokorny et al. model (Figure 2.6).

6.3 Gamut sizes and colour differences

We observed smaller color gamuts for the old observers relative to the young observer, without or with full/partial adaptation. A previous investigation on using the FM100 Hue test to assess the colour rendering properties of lights with a correlated colour temperature of approximately 3500K found no evidence that a smaller gamut area was associated with poorer chromatic discrimination (Esposito and Houser, 2017). Our results agree, providing that adaptation takes place to some degree. However, if the gamut contracts appreciably as it did with the no adaptation condition, then the TES of the FM100 will increase.

With both complete and partial adaptation, the gamut area for the older observers shows an asymmetric reduction from the young. This trend continues with no adaptation, and there is a shift of the colours in the vertical direction. Generally, if there is a uniform reduction in the gamut around the white point, colours appear less saturated with minimal changes in hue. Our results showed an asymmetrical reduction in the gamut when the adaptation factor was reduced, suggesting that colours such as blue and purple become more desaturated, but the saturation of green, yellow, and red remains constant. Without adaptation, the observed vertical shift represents a change in the white point towards yellow. The yellow shift also causes the bluish caps to appear less blue and shifts the greens toward yellowish green and red to orange. Thus, the bluish caps become less blue, and yellowish caps become more yellowish in appearance, respectively.

Overall, the colour differences (ΔE) observed between adjacent caps of the FM100 Hue test for the young and old observers ranged from $0.19 \leq \Delta E \leq 3.05$ for viewing conditions with adaptation, partial adaptation and without adaptation. Typically, observers should not notice any difference for caps ranging $0 < \Delta E < 1$. Experienced observers are likely to notice the colour difference within the range $1 < \Delta E < 2$, while inexperienced observers begin to notice colour difference within the range $2 < \Delta E < 3.5$ (Mokrzycki and Tatol, 2011). Because we assumed an ideal observer, we assumed that all observers were experienced. There were occasions where the ΔE_1 was less than 1.0; however, this did not affect the order between the caps because the ΔE_2 was above 1.0, so that ordering based on similarity would be the correct order, and no transposition would occur. For an inexperienced observer, the error score would increase as would the variability in the error score since there are more possible arrangements, but the relative difficulty of the trays would be the same.

The gamut area may not be the best index for colour discrimination, but in this data, we show that the colour differences decrease with the reduction in gamut area. Although different colour spaces were used to calculate the differences between adjacent caps, both Lakowski's analysis and ours showed the mean difference across trays were similar, indicating that, on average, the FM100 spacing is perceptually uniform. However, our rank order of difficulty based on the mean colour differences differed between the two

studies. Based on Lakowski's mean colour difference data, the most difficult tray would be tray 3, followed by trays 2, 4 and 1. Our mean colour difference data suggests that tray 1 would be most challenging to arrange, followed by trays 2, 4, and 3. The discrepancy in rank order could be a result of small differences in reflectance properties of the caps, the different reference white lights that were used (Illuminant C vs D65), differences in the accuracy of the equipment used to measure the cap reflectances or any combination of these factors.

The non-uniformities in the cap spacing become more apparent when caps are grouped by the blue-yellow and red-green quadrants. This grouping shows that the colour differences are smaller in the blue-yellow region of the FM100 and explains why real observers have higher blue-yellow partial error scores (Smith et al., 1985; Kinnear and Sahraie, 2002).

6.4 Limitations of the study

First, we assumed ideal observers with a colour difference threshold implicitly set to a $\Delta E=1.0$. Thus, there is no variability in the TES within age-category and no change in the chromatic sensitivity with age. To increase the variability and be more realistic with data, the threshold for small colour differences could be increased to a value greater than 1.0 to increase the number of possible arrangements and thereby increase the variability and mean TES within each age category. Increasing the chromatic threshold also raises the question as to whether to increase the threshold of the older observer more than the younger observer. Increasing the older observer's threshold by the same amount could increase the BY error scores more than the RG error scores because the average colour difference for the BY quadrants is less for the older observer regardless of the degree of adaptation. These questions can be investigated further in future modeling research using the FM100 Hue Test.

Second, we looked at only one colour vision model with one adaptation mechanism. We are not certain how other colour vision models would perform or what adaptation adjustments would be required. Other approaches might be less complex but would still show the same trends as observed in this study.

Third, by looking at only two ages, our data suggest that there is a linear increase in the FM100 scores with age. We do not know if the model predicts the same non-linear trend as shown in the clinical data.

6.5 Conclusion

Our study objective was to examine the theoretical changes in the FM100 Hue scores produced by age-related changes in the ocular media transmittances older ideal observers. We found different patterns of cap arrangement among the older observers with or without adaptation in place.

With complete and partial chromatic adaptation (D = 1, and D=0.67), the TES increased from 8 in the younger observers to 12 for older observers; however, the increase in the total error score was as a result of an increase in the red-green partial error score and not the blue-yellow. Without adaptation, the predicted TES for the older observers increased further. The TES values were greater, i.e., 16 (RG 12, BY 4) and 20 (RG 12, BY 8) for van de Kraats' and van Norren's observer and Pokorny et al.'s observer, respectively. Transpositions in trays 3 and 4 accounted for all the errors among all the observers, with tray 3 having the greater share. There were no predicted errors in trays 1 and 2, which contain red to red-orange and yellow to yellow-green hues, respectively.

Our results show that the von Kries-type chromatic adaptation, as applied in the CIECAM02 colour space, improves hue discrimination in the aged eye. The von Kries-type chromatic adaptation can potentially counteract the effects of age-related changes in the ocular media; however, this improvement does not match the hue discrimination level of the young adult.

The outcome of this study could set a good stage for future research to in modeling the non-uniformity of age-related changes in chromatic discrimination along the blue-yellow and red-green axis using the FM100 Hue test. The future studies could provide a method for adjusting the FM100 Hue TES to account for media absorption, by which one would quantify the age-related neural changes on chromatic discrimination using the FM100 test.

References

Ahnelt, P. K., Kolb, H. & Pflug, R. 1987. Identification of a subtype of cone photoreceptor, likely to be blue sensitive, in the human retina. *J Comp Neurol,* 255**,** 18-34.

Artal, P., Guirao, A., Berrio, E., Piers, P. & Norrby, S. 2003. Optical aberrations and the aging eye. *Int Ophthalmol Clin,* 43**,** 63-77.

Barbur, J. L. & Rodriguez-Carmona, M. 2015. Color vision changes in normal aging. *In:* ELLIOT, A. J., FRANKLIN, A. & FAIRCHILD, M. D. (eds.) *Handbook of Color Psychology.* Cambridge: Cambridge University Press.

Beirne, R. O., Mcilreavy, L. & Zlatkova, M. B. 2008. The effect of age-related lens yellowing on Farnsworth-Munsell 100 hue error score. *Ophthalmic Physiol Opt,* 28**,** 448-56.

Birch, J. 2012. Worldwide prevalence of red-green color deficiency. *Journal of the Optical Society of America. A, Optics, image science, and vision,* 29**,** 313-20.

Boettner, E. A. & Wolter, J. R. 1962. Transmission of the Ocular Media. *Investigative ophthalmology & visual science,* 1**,** 776.

Burns, S. A., Smith, V. C., Pokorny, J. & Elsner, A. E. 1982. Brightness of equal-luminance lights. *Journal of the Optical Society of America,* 72**,** 1225-1231.

Commission Internationale de l'Eclairage. 2004. Technical Report: A Colour Appearance Model for Colour Management Systems: CIECAM02.

Commission Internationale de l'Eclairage. 2020a. e-ILV: International Lighting Vocabulary 2nd ed. Vienna.

Commission Internationale de l'Eclairage. 2020b. Colorimetry - Part 2: CIE Standard illuminants. *CIE ISO DIS 11664-2 : Vienna 2020.*

Cionni, R. J. & Tsai, J. H. 2006. Color perception with AcrySof Natural and AcrySof single-piece intraocular lenses under photopic and mesopic conditions. *Journal of Cataract & Refractive Surgery,* 32**,** 236-242.

Canadian Ophthalmological Society. 2008. Correspondence of 11 April, 2008. Cited on January 20, 2021.

Curcio, C. A., Allen, K. A., Sloan, K. R., Lerea, C. L., Hurley, J. B., Klock, I. B. & Milam, A. H. 1991. Distribution and morphology of human cone photoreceptors stained with anti-blue opsin. *Journal of comparative neurology (1911),* 312**,** 610-624.

Curcio, C. A. & Drucker, D. N. 1993. Retinal ganglion cells in Alzheimer's disease and aging. *Ann Neurol,* 33**,** 248-57.

Curcio, C. A., Millican, C. L., Allen, K. A. & Kalina, R. E. 1993. Aging of the human photoreceptor mosaic: evidence for selective vulnerability of rods in central retina. *Invest Ophthalmol Vis Sci,* 34**,** 3278-96.

Dain, S. J. 2004. Clinical colour vision tests. *Clin Exp Optom,* 87**,** 276-93.

Dain, S. J., Atchison, D. A. & Hovis, J. K. 2019. Limitations and Precautions in the Use of the Farnsworth-Munsell Dichotomous D-15 Test. *Optometry and vision science : official publication of the American Academy of Optometry,* 96**,** 695-705.

Dain, S. J., Cassimaty, V. T. & Psarakis, D. T. 2004. Differences in FM100-Hue test performance related to iris colour may be due to pupil size as well as presumed amounts of macular pigmentation. *Clin Exp Optom,* 87**,** 322-5.

Dain, S. J., Pereira, S., Palmer, B., Lewis, P. & Hammond, T. 1980. *Illuminance and the FM100 Hue Test*.

De Valois, R. L. & De Valois, K. K. 1993. A multi-stage color model. *Vision Res,* 33**,** 1053-65.

Eisner, A., Fleming, S. A., Klein, M. L. & Mauldin, W. M. 1987. Sensitivities in older eyes with good acuity: cross-sectional norms. *Investigative Ophthalmology & Visual Science,* 28**,** 1824-1831.

Esposito, T. 2019. An Adjusted Error Score Calculation for the Farnsworth-Munsell 100 Hue Test. *LEUKOS,* 15**,** 195-202.

Esposito, T. & Houser, K. 2017. A new measure of colour discrimination for LEDs and other light sources. *Lighting Research & Technology,* 51**,** 147715351772920.

Fairchild, M. D. 2013. *Color Appearance Models,* New York, John Wiley & Sons, Incorporated.

Farnsworth, D. 1949. *The Farnsworth-Munsell 100 hue test for the examination of colour vision*, Baltimore: Munsell color company.

Gao, H. & Hollyfield, J. G. 1992. Aging of the human retina. Differential loss of neurons and retinal pigment epithelial cells. *Invest Ophthalmol Vis Sci,* 33**,** 1-17.

Gaska, J., Winterbottom, M. & Atta, V. A. 2016. Operational Based Vision Assessment Cone Contrast Test: Description and Operation. SCHOOL OF AEROSPACE MEDICINE WRIGHT-PATTERSON AFB OH.

Gipson, I. K. 2013. Age-Related Changes and Diseases of the Ocular Surface and Cornea. *Investigative Ophthalmology & Visual Science,* 54**,** ORSF48-ORSF53.

Guth, S. L. 1991. Model for color vision and light adaptation. *Journal of the Optical Society of America A,* 8**,** 976-993.

Guth, S. L. 1992. Model for color vision and light adaptation: erratum. *Journal of the Optical Society of America A,* 9**,** 344-344.

Guth, S. L., Massof, R. W. & Benzschawel, T. 1980. Vector model for normal and dichromatic color vision. *Journal of the Optical Society of America (1930),* 70**,** 197-212.

Haegerstrom-Portnoy, G. 1988. Short-wavelength-sensitive-cone sensitivity loss with aging: a protective role for macular pigment? *Journal of the Optical Society of America A,* 5**,** 2140-2144.

Hendrickson, A., Possin, D., Vajzovic, L. & Toth, C. A. 2012. Histologic development of the human fovea from midgestation to maturity. *Am J Ophthalmol,* 154**,** 767-778.e2.

Hendrickson, A. E. & Yuodelis, C. 1984. The morphological development of the human fovea. *Ophthalmology,* 91**,** 603-12.

Hurvich, L. M. & Jameson, D. 1955. Some quantitative aspects of an opponent-colors theory. II. Brightness, saturation, and hue in normal and dichromatic vision. *Journal of the Optical Society of America (1930),* 45**,** 602.

Jackson, G. R., Owsley, C. & Curcio, C. A. 2002. Photoreceptor degeneration and dysfunction in aging and age-related maculopathy. *Aging Res Rev,* 1**,** 381-96.

Jameson, D. & Hurvich, L. M. 1955. Some Quantitative Aspects of an Opponent-Colors Theory I Chromatic Responses and Spectral Saturation. *Journal of the Optical Society of America (1930),* 45**,** 546.

Kinnear, P. R. 1970. Proposals for scoring and assessing the 100-Hue test. *Vision Res,* 10**,** 423-33.

Kinnear, P. R. & Sahraie, A. 2002. New Farnsworth-Munsell 100 hue test norms of normal observers for each year of age 5-22 and for age decades 30-70. *Br J Ophthalmol,* 86**,** 1408-11.

Knoblauch, K., Saunders, F., Kusuda, M., Hynes, R., Podgor, M., Higgins, K. E. & De Monasterio, F. M. 1987. Age and illuminance effects in the Farnsworth-Munsell 100-hue test. *Appl Opt,* 26**,** 1441-8.

Knoblauch, K., Vital-Durand, F. & Barbur, J. L. 2001. Variation of chromatic sensitivity across the life span. *Vision Res,* 41**,** 23-36.

Lakowski, R. 1962. Is the deterioration of colour discrimination with age due to lens or retinal change? *Farbe,* 2**,** 69-86.

Lakowski, R. 1966. A critical evaluation of colour vision tests. *Br J Physiol Opt,* 23**,** 186-209.

Lennie, P., Pokorny, J. & Smith, V. C. 1993. Luminance. *Journal of the Optical Society of America. A, Optics and image science,* 10**,** 1283.

Luo, M., Cui, G. & Changjun, L. 2006. Uniform colour spaces based on CIECAMO2 colour appearance model. *Color Research & Application,* 31**,** 320-330.

Mantyjarvi, M. 2001. Normal test scores in the Farnsworth-Munsell 100 hue test. *Doc Ophthalmol,* 102**,** 73-80.

Mäntyjärvi, M., Syrjäkoski, J., Tuppurainen, K. & Honkonen, V. 1997. Colour vision through intraocular lens. *Acta Ophthalmol Scand,* 75**,** 166-9.

Mäntyjärvi, M. & Tuppurainen, K. 1996. Color vision in patients with a silicone intraocular lens. *J Cataract Refract Surg,* 22 Suppl 2**,** 1308-12.

Mokrzycki, W. & Tatol, M. 2011. Color difference Delta E - A survey. *Machine Graphics and Vision,* 20**,** 383-411.

Moroney, N., Fairchild, M., Hunt, R., Changjun, L., Luo, M. & Newman, T. 2002a. *The CIECAM02 color appearance model*.

Moroney, N., Fairchild, M. D., Hunt, R. W., Li, C., Luo, M. R. & Newman, T. The CIECAM02 color appearance model. Color and Imaging Conference, 2002b. Society for Imaging Science and Technology, 23-27.

Neitz, J. & Neitz, M. 2011. The genetics of normal and defective color vision. *Vision research,* 51**,** 633-651.

Neitz, M. & Neitz, J. 2000. Molecular Genetics of Color Vision and Color Vision Defects. *Archives of Ophthalmology,* 118**,** 691-700.

Neitz, M. & Neitz, J. 2010. Chapter 62 - Color vision defects. *In:* LEVIN, L. A. & ALBERT, D. M. (eds.) *Ocular Disease.* Edinburgh: W.B. Saunders.

Neitz, M., Neitz, J. & Grishok, A. 1995. Polymorphism in the number of genes encoding long-wavelength-sensitive cone pigments among males with normal color vision. *Vision research,* 35**,** 2395-2407.

Owsley, C. 2011. Aging and vision. *Vision Res,* 51**,** 1610-22.

Paramei, G. V. & Oakley, B. 2014. Variation of color discrimination across the life span. *J Opt Soc Am A Opt Image Sci Vis,* 31**,** A375-84.

Pinckers, A. 1980. Color vision and age. *Ophthalmologica,* 181**,** 23-30.

Pokorny, J. & Smith, V. C. 1976. Effect of field size on red--green color mixture equations. *J Opt Soc Am,* 66**,** 705-8.

Pokorny, J., Smith, V. C. & Lutze, M. 1987. Aging of the human lens. *Applied Optics,* 26**,** 1437-1440.

Pokorny, J., Smith, V. C., Verriest, G. & Pinckers, A. J. L. G. 1979. *Congenital and Acquired Color Vision Defects,* New York Grune & Stratton.

Roy, M. S., Podgor, M. J., Collier, B. & Gunkel, R. D. 1991. Color vision and age in a normal North American population. *Graefe's Archive for Clinical and Experimental Ophthalmology,* 229**,** 139-144.

Ruddock, K. H. 1965. The effect of age upon colour vision. II. Changes with age in light transmission of the ocular media. *Vision Res,* 5**,** 47-58.

Rushton, W. A. 1972. Pigments and signals in colour vision. *The Journal of physiology,* 220**,** 1P-31P.

Schneck, M. E., Haegerstrom-Portnoy, G., Lott, L. A. & Brabyn, J. A. 2014. Comparison of panel D-15 tests in a large older population. *Optom Vis Sci,* 91**,** 284-90.

Shevell, S. K., He, J. C., Kainz, P., Neitz, J. & Neitz, M. 1998. Relating color discrimination to photopigment genes in deutan observers. *Vision Research,* 38**,** 3371-3376.

Shinomori, K., Panorgias, A. & Werner, J. S. 2016. Discrimination thresholds of normal and anomalous trichromats: Model of senescent changes in ocular media density on the Cambridge Colour Test. *Journal of the Optical Society of America. A, Optics, image science, and vision,* 33**,** A65-A76.

Sloan, L. L. 1940. INSTRUMENTS AND TECHNICS FOR THE CLINICAL TESTING OF LIGHT SENSE: IV. SIZE OF PUPIL AS A VARIABLE FACTOR IN THE DETERMINATION OF THE LIGHT MINIMUM. *Archives of Ophthalmology,* 24**,** 258-275.

Smet, K. a. G., Zhai, Q., Luo, M. R. & Hanselaer, P. 2017. Study of chromatic adaptation using memory color matches, Part II: colored illuminants. *Optics Express,* 25**,** 8350-8365.

Smith, V. C., Pokorny, J. & Pass, A. S. 1985. Color-axis determination on the Farnsworth-Munsell 100-hue test. *Am J Ophthalmol,* 100**,** 176-82.

Suryakumar, R. & Allison, R. 2016. Accommodation and pupil responses to random-dot stereograms. *Journal of optometry,* 9**,** 40-46.

Swanson, W. H. & Fish, G. E. 1996. Age-related changes in the color-match-area effect. *Vision Res,* 36**,** 2079-85.

Tekavcic Pompe, M. & Stirn Kranjc, B. 2012. Which psychophysical colour vision test to use for screening in 3–9 year olds? *Zdravstveni vestnik,* 81**,** 170-177.

Van De Kraats, J. & Van Norren, D. 2007. Optical density of the aging human ocular media in the visible and the UV. *J Opt Soc Am A Opt Image Sci Vis,* 24**,** 1842-57.

Van Den Berg, T. J. & Tan, K. E. 1994. Light transmittance of the human cornea from 320 to 700 nm for different ages. *Vision Res,* 34**,** 1453-6.

Verriest, G. 1963. Further studies on acquired deficiency of color discrimination. *J Opt Soc Am,* 53**,** 185-95.

Verriest, G., Van Laethem, J. & Uvijls, A. 1982. A new assessment of the normal ranges of the Farnsworth-Munsell 100-hue test scores. *Am J Ophthalmol,* 93**,** 635-42.

Volbrecht, V. J., Shrago, E. E., Schefrin, B. E. & Werner, J. S. 2000. Spatial summation in human cone mechanisms from 0 degrees to 20 degrees in the superior retina. *Journal of the Optical Society of America. A, Optics, image science, and vision,* 17**,** 641-650.

Vuori, M. L. & Mäntyjärvi, M. 2006. Colour vision and retinal nerve fibre layer photography in patients with an Acrysof® Natural intraocular lens. *Acta Ophthalmologica Scandinavica,* 84**,** 92-94.

Weale, R. A. 1988. Age and the transmittance of the human crystalline lens. *The Journal of physiology,* 395**,** 577-587.

Werner, J. S. 2016. The Verriest Lecture: Short-wave-sensitive cone pathways across the life span. *Journal of the Optical Society of America. A, Optics, image science, and vision,* 33**,** A104-A122.

Wheatley, W. & Spitschan, M. version Oct 30, 2018 *Watson & Yellott's (2012) unified formula for light-adapted pupil size* [Online]. Available: https://github.com/spitschan/WatsonYellott2012_PupilSize [Accessed March, 20th 2021].

Winn, B., Whitaker, D., Elliott, D. B. & Phillips, N. J. 1994. Factors affecting light-adapted pupil size in normal human subjects. *Investigative Ophthalmology & Visual Science,* 35**,** 1132-1137.

Wyszecki, G. N. & Stiles, W. S. 1982. *Color science : concepts and methods, quantitative data and formulae,* New York ;, Wiley.